S-N Fatigue Design and Test Data for Low-Alloy Steel Bolts

API TECHNICAL REPORT 21TR2
SECOND EDITION, JULY 2025

American
Petroleum
Institute

Special Notes

API publications necessarily address problems of a general nature. With respect to particular circumstances, local, state, and federal laws and regulations should be reviewed. The use of API publications is voluntary. In some cases, third parties or authorities having jurisdiction may choose to incorporate API standards by reference and may mandate compliance.

Neither API nor any of API's employees, subcontractors, consultants, committees, or other assignees make any warranty or representation, either express or implied, with respect to the accuracy, completeness, or usefulness of the information contained herein, or assume any liability or responsibility for any use, or the results of such use, of any information or process disclosed in this publication. Neither API nor any of API's employees, subcontractors, consultants, or other assignees represent that use of this publication would not infringe upon privately owned rights.

API publications may be used by anyone desiring to do so. Every effort has been made by the Institute to ensure the accuracy and reliability of the data contained in them; however, the Institute makes no representation, warranty, or guarantee in connection with this publication and hereby expressly disclaims any liability or responsibility for loss or damage resulting from its use or for the violation of any authorities having jurisdiction with which this publication may conflict.

API publications are published to facilitate the broad availability of proven, sound engineering and operating practices. These publications are not intended to obviate the need for applying sound engineering judgment regarding when and where these publications should be used. The formulation and publication of API publications is not intended in any way to inhibit anyone from using any other practices.

Any manufacturer marking equipment or materials in conformance with the marking requirements of an API standard is solely responsible for complying with all the applicable requirements of that standard. API does not represent, warrant, or guarantee that such products do in fact conform to the applicable API standard.

Classified areas may vary depending on the location, conditions, equipment, and substances involved in any given situation. Users of this technical report (TR) should consult with the appropriate authorities having jurisdiction.

Users of this TR should not rely exclusively on the information contained in this document. Sound business, scientific, engineering, and safety judgment should be used in employing the information contained herein.

Foreword

Nothing contained in any API publication is to be construed as granting any right, by implication or otherwise, for the manufacture, sale, or use of any method, apparatus, or product covered by letters patent. Neither should anything contained in the publication be construed as insuring anyone against liability for infringement of letters patent.

Suggested revisions are invited and should be submitted to the Standards Department, API, 200 Massachusetts Avenue NW, Suite 1100, Washington, DC 20001, standards@api.org.

Contents

Figures

Contents

Page

Tables

Introduction

The requirements for bolting fatigue assessment were a charge of the API CSOEM Multi-Segment Task Group on Bolting Failures. Due to documented subsea bolting failures defined in the BSEE QC-FIT Evaluation of Connector and Bolt Failures, the charge of the sub-task group TGR-13 was the following:

"*Guidance should be issued by API on when and how to perform fatigue sensitivity analysis on bolting*."

API CSOEM Bolting Report for TGR-13 and TGR-14 was issued. It defined the design guidelines and provided recommendations for performing a full-scale fatigue testing on bolting. Upon further approval, full-scale fatigue testing was performed.

The scope of work was conducted in two phases; Phase I: Evaluation of bolting under cyclic loading which meets the requirements of API 17D:2011, 2nd Edition [1] standard and Phase II: Evaluation of bolting which meets the requirements of API 6A/16A [2, 3] standards. The following guidelines are provided for both design verification fatigue analysis and corresponding full-scale fatigue testing that was performed.

Design verification analysis for fatigue assessment of bolting requires an evaluation for S-N (stress number of cycles to failure) or fatigue crack growth rate. The S-N fatigue evaluation can be based on either the stress concentrations of the thread profile, which will need stress concentration factor (SCF) and smooth tensile bar S-N testing, or the axial stress due to the load divided by the minimum root diameter area and full-scale bolt fatigue tests [4]. The basis of this document is the S-N approach using full-scale fatigue testing. The full-scale fatigue testing was conducted for bolts manufactured to meet API 20E [4] BSL-3. The testing was performed in two phases; Phase I was conducted to obtain S-N fatigue curve with API 17D:2011 loading conditions, Phase II was conducted with API 6A/16A loading conditions.

The fatigue testing was based on alternating axial stresses in the bolt with a defined preload. The preload was applied with the load frame to a value of 2/3*SMYS for Phase I testing and 0.5*SMYS for Phase II testing, based on the cross section at the root radius of the thread. The defined bolt lengths represent API flange by flange connection conservative bolt lengths for a given bolt size. The bolt-to-nut thread engagement met the requirements of API 6A for all tests. Each bolt tested had two bolt/nut connections where the failure of the first connection was defined as the fatigue life.

The objective of the Phase I test program was to provide S-N fatigue curves for bolts that are preloaded per API Series 17 standards and are subjected to a range of alternating axial stresses. The objective of the Phase II test program was to provide S-N fatigue curves for bolts that are preloaded per API 6A/16A standards. The preload and alternating stress ranges were defined based on the cross-sectional area at the root radius of the threads. The test program evaluated bolt size effects and environments of air and saltwater (SW) with cathodic protection (CP).

S-N Fatigue Design and Test Data for Low-Alloy Steel Bolts

1 Scope

The scope of the test program was to obtain bolting material fatigue data required to perform design verification analysis of bolting subjected to fatigue loading to assure accurate design life estimation. The bolting fatigue testing program provided S-N fatigue curves for three alternating stress ranges in air and in SW+CP environments and for bolt sizes of 1 in., 2 in. (Grade L7), and 3 in. (Grade L43) in Phase I and for bolt sizes 1 in. (Grade L7) and 3 in. (Grade L43) in Phase II.

The results of these S-N fatigue tests allow the bolting design to be assessed for S-N fatigue through structural analysis using the nominal root area stresses in the bolt, avoiding the need to define stress and load concentrations in the bolt root radius of engaged threads.

The design guidelines and the fatigue data provided in the document are intended to be used for bolting with unified national thread with root radius (UNR) specifications of ASME B1.1 [5] Class 2A/2B.

2 Normative References

There are no normative references for this document.

3 Terms, Definitions, Abbreviations, and Symbols

3.1 Terms and Definitions

For the purposes of this document, the following definitions apply.

3.1.1
ambient air (dry)
Room temperature and ambient pressure.

3.1.2
high-stress range fatigue cycles
HFC
Tested fatigue cycles to failure for a high-stress range or high-force condition applied.

3.1.3
low-stress range fatigue cycles
LFC
Tested fatigue cycles to failure for a low-stress range or low-force condition applied.

3.1.4
mean stress
Maximum axial stress plus minimum axial stress divided by two.

3.1.5
medium-stress range fatigue cycles
MFC
Tested fatigue cycles to failure for a medium-stress range or medium-force condition applied.

3.1.6
S-N fatigue
Stress range (S) versus number of cycles to failure (N).

3.1.7
stress range
The difference between the maximum axial stress and minimum axial stress being applied.

3.2 Abbreviations

CP	cathodic protection
EF	electric furnace
EDS	energy dispersive X-ray spectroscopy
HFC	high-stress range fatigue cycles
FSF	full-scale fatigue
LFC	low-stress range fatigue cycles
MFC	medium-stress range fatigue cycles
MPS	manufacturing process specification
SAF	stress amplification factor
SCE	saturated calomel electrode
SCF	stress concentration factor
SD	standard deviation
SEM	scanning electron microscopy
SMYS	specified minimum yield strength
S-N	stress-number of cycles to failure
SW	saltwater
UNR	unified national thread with root radius
YS	yield strength

3.3 Symbols

N	is the number of cycles to failure
a	is the intercept of design S-N curve with the log N axis
m	is the negative inverse slope of the S-N curve
t_p	ASTM E739 scaling factor based on 95 % confidence level
$\Delta\sigma$	stress range

4 Bolting Fatigue Analysis Design Guidelines

4.1 Bolting Subjected to Cyclic Loading

Bolting subjected to cyclic loading can typically include the bolts and nuts for flanged connections, bolts that are threaded directly into components, and bolts for clamp connections.

Bolting that transfers loads of the riser systems to the wellhead can be considered fatigue-sensitive and be evaluated for cyclic loading. This includes cyclic loadings from drilling risers, workover/completion risers, and production risers. Other bolting may require fatigue evaluation depending on the operating conditions and the load path.

4.2 Bolting S-N Fatigue Analysis Procedure

Fatigue-sensitive bolts using unified screw threads can be designed and analyzed per these methods. The steps for the bolt fatigue analysis using the S-N test data available in this document are defined as:

1) The evaluation of the connection for fatigue alternating stresses is to be performed without modeling the threads, as the fatigue curves have been defined based on full-scale bolt fatigue testing, as presented in Section 5. The bolt fatigue stress analysis, without the threads modeled, can be conducted using linear elastic material properties. The minimum specified yield strength outlined in API 17D:2011, 2nd Edition (Phase I) and API 6A/16A (Phase II) suite of documents can be used for the analysis.

2) Apply the bolt preload to a minimum of 67 % of bolt yield strength (Phase I) or 50 % of yield strength (Phase II).

3) Apply the applicable loads. The analysis of bolting for fatigue will define the alternating stresses in the highest loaded bolt of the component for defined cyclic loads of pressure, temperature, and external loads. The maximum stress of the alternating stress range cannot exceed the allowable axial stress limit as defined in the API Subcommittee 17 (Phase I) and API 6A/16A (Phase II) suite of standards. Both axial and bending stresses in the bolt can be considered for the fatigue evaluation. Bolt bending loads can be converted to equivalent tension loads and combined with the axial loads to define the total alternating stress range. Finite element analysis of the bolting will define a location that has the minimum and maximum axial membrane plus bending stresses without discontinuities or stress concentrations to determine the maximum alternating stress range [6].

   NOTE Bending or a combination of alternating tension plus bending would result in conservative values [7].

   Combinations of internal pressure, external bending/tension, and thermal-induced cyclic loads can be evaluated for fatigue of the bolting. Thermal loads may be evaluated for both thermal expansion/contraction loads that result in external load of the connection and the thermal expansion of the connection, which produces direct loads on the bolting.

4) Calculate the stress range for the bolt. The stress range due to cyclic load is defined as maximum axial membrane minus the minimum axial membrane plus bending stress due to bolt preload plus all cyclic loading defined based on minimum root area of the bolts, for a defined location.

5) Using the stress range, calculate the fatigue life for the bolt using the S-N test data in Section 5. The stress range of the bolt shank is the stress value to define the total cycles to failure for a given environment based on full-scale test data. No mean stress correction for applying this method is necessary. Palmgren-Miner‘s rule can be used for accumulated damage for assessing different cyclic load cases.

   It is most appropriate to have the bolts being assessed have the same parameters as the bolts that were used in the full-scale fatigue testing in Section 5. Key parameters are the thread form, thread processing, material, material properties, material processing, and bolt preload. Interpolation of fatigue curves is acceptable for bolt diameter sizes between 1 in. and 3 in., having an 8-UNR thread profile.

5 Full-Scale Fatigue Test Data for Bolting

5.1 Bolting Materials

5.1.1 General

Three sizes (1 in., 2 in., and 3 in.) of bolts and nuts in Phase I and two sizes of (1 in. and 3 in.) low-alloy steel bolts and nuts in Phase II were used for conducting the full-scale fatigue (FSF) testing. Table 1 provides the bolt and nut sizes, materials, and corresponding standards.

Table 1—Bolts and Nuts used for Phase I and Phase II of FSF Testing [8, 9]

Bolt Size, (in.)	Bolt Material and Corresponding Standards	Nut Size (in.) Heavy Hex	Nut Material and Corresponding Standards
1 (8 UNCR Class 2A)	ASTM A320, Grade L7	1 (8 UNCR Class 2B)	ASTM A194, Grade 7L
2 (8 UNR Class 2A)	ASTM A320, Grade L7	2 (8 UNR Class 2B)	ASTM A194, Grade 7L
3 (8 UNR Class 2A)	ASTM A320, Grade L43	3 (8 UNR Class 2B)	ASTM A194, Grade 7L

All bolts and nuts were manufactured in accordance with API 20E BSL-3. Two heats from each bolt size were procured from two different manufacturers, defined as Supplier 1 (Heat 1) and Supplier 2 (Heat 2). For each size, 23 bolts and 41 nuts in Phase I; 20 bolts and 40 nuts in Phase II were procured from each manufacturer.

5.1.2 Manufacturing Procedure

The low-alloy steel raw material was produced by electric furnace (EF) with secondary refinement using vacuum degassing. Hot rolled bars were heat treated to the targeted mechanical strength then machined to the specific sizes of bolts and nuts. Prior to the production, the manufacturing process specifications (MPS) from each supplier was reviewed and approved by the API technical team for this project.

All the threads were machined (cut) threads. The Heat 1 bolts were double-ended studs, and the Heat 2 bolts were full-threaded bolts. All the nuts from Heat 1 (Supplier 1) were forged while the nuts from Heat 2 (Supplier 2) were machined from bar stock.

5.1.3 Chemical Compositions

Heat numbers, reduction ratio from hot working, and chemical compositions of the bolts and nuts for Phase I and Phase II are given in Tables 2 and 3, respectively.

Table 2—Bolt and Nut Heat Numbers, Reduction Ratios, and Chemical Compositions (Phase I)

Bolt Heats	Heat No.	Forged Bar RR	Bolt/Nut	C	Mn	P	S	Si	Cr	Mo	B	Ni
Manufacturer 1	H1-1	788:1	1-in. bolt	0.41	0.97	0.011	0.003	0.23	1.03	0.2	0.0004	—
	H1-2 (31 off)	378:1	1-in. nut	0.42	0.97	0.008	0.007	0.28	0.98	0.2	0.0002	—
	H1-3 (10 off)	443:1	1-in. nut	0.41	0.97	0.008	0.01	0.25	0.98	0.20	0.0002	—
	H1-4	159.7:1	2-in. bolt	0.41	0.98	0.007	0.007	0.30	1.07	0.15	0.0002	—
	H1-5	132:1	2-in. nut	0.41	0.97	0.008	0.001	0.26	0.98	0.20	0.0002	—
	H1-6	102.2:1	3-in. bolt	0.41	0.78	0.009	0.002	0.25	0.87	0.27	0.0002	1.79
	H1-7	49.3:1	3-in. nut	0.41	0.98	0.008	0.005	0.27	0.99	0.2	0.0002	—
Manufacturer 2	H2-1	189.8:1	1-in. bolt	0.41	0.86	0.008	0.002	0.29	1.09	0.25	0.0002	—
	H2-2	109.6:1	1-in. nut	0.40	0.88	0.008	0.002	0.34	1.01	0.23	0.0003	—
	H2-3	76.1:1	2-in. bolt	0.40	0.88	0.008	0.002	0.34	1.01	0.23	0.0003	—
	H2-4	27.4:1	2-in. nut	0.41	0.88	0.007	0.003	0.27	1.03	0.24	0.0004	—
	H2-5	34.6:1	3-in. bolt	0.40	0.74	0.007	0.004	0.28	0.82	0.3	0.0003	1.91
	H2-6	34.6:1	3-in. bolt	0.40	0.74	0.007	0.004	0.28	0.82	0.3	0.0003	1.91
	H2-7	14:1	3-in. nut	0.41	0.88	0.007	0.003	0.27	1.03	0.24	0.0004	—

Table 3—Bolts and Nuts Heat Numbers, Reduction Ratios, and Chemical Compositions (Phase II)

Bolt Heats	Heat No.	Forged Bar RR	Bolt/Nut	C	Mn	P	S	Si	Cr	Mo	B	Ni
Manufacturer 1	H1-1	788.7:1	1-in. bolt	0.41	0.94	0.008	0.003	0.23	1.04	0.21	0.0002	—
	H1-2	443.7:1	1-in. nut	0.41	0.94	0.012	0.002	0.21	1.02	0.20	0.0001	—
	H1-3	102.2:1	3-in. bolt	0.41	0.78	0.009	0.002	0.25	0.87	0.27	0.0002	1.79
	H1-4	49.2:1	3-in. nut	0.42	0.97	0.009	0.004	0.22	0.99	0.21	0.0002	—
Manufacturer 2	H2-1	—	1-in. bolt	0.40	0.90	0.009	0.001	0.33	1.03	0.23	0.0004	0.23
	H2-2	—	1-in. nut	0.41	0.89	0.007	0.004	0.35	1.03	0.21	0.0005	0.21
	H2-3	—	3-in. bolt	0.40	0.80	0.008	0.013	0.24	0.82	0.27	0.0004	1.89
	H2-4	—	3-in. nut	0.4	0.9	0.009	0.001	0.33	1.03	0.23	0.0004	0.23

5.1.4 Heat Treatment

Heat treatment conditions of the bolts and nuts performed by the manufacturers prior to machining for Phase I and Phase II are given in Tables 4 and 5, respectively.

Table 4—Heat Treatment Details of the Bolts and Nuts Prior to Machining (Phase I)

Bolt Heats	Heat No.	Bolt/ Nut	Normalizing			Austenitizing			Tempering		
			Temp °F	Time h	Cooling Media	Temp °F	Time h	Cooling Media	Temp. °F	Time h	Cooling Media
Manufacturer 1	H1-1	1-in. bolt	1650	2.5	Air	1575	2.5	Polymer	1160	3.0	Water
	H1-2 (31 off) and H1-3 (10 off)	1-in. nut	1650	2.5	Air	1550	2.5	Polymer	1160	3.0	Water
	H1-4 (10 off)	2-in. bolt	1650	3.0	Air	1575	3.0	Polymer	1160	3.5	Water
	H1-5	2-in. nut	1650	3.0	Air	1550	3.0	Polymer	1160	3.5	Water
	H-6	3-in. bolt	1650	3.0	Air	1575	3.0	Oil	1st: 1165 2nd: 1115	3.5 3.5	Water Water
	H1-7	3-in. nut	1650	3.5	Air	1550	3.5	Polymer	1160	3.5	Water
Manufacturer 2	H2-1	1-in. bolt	—	—	—	1580	1.67	Oil	1148	2.33	Polymer
	H2-2	1-in. nut	—	—	—	1580	1.5	Oil	1148	2.33	Polymer
	H2-3	2-in. bolt	—	—	—	1580	1.67	Oil	1148	2.33	Polymer
	H2-4	2-in. nut	—	—	—	1580	1.5	Oil	1148	2.33	Polymer
	H2-5 (11 off)	3-in. bolt	—	—	—	1580	1.67	Oil	1st: 1148 2nd: 1148	2.5 2.5	Polymer Polymer
	H2-6 (12 off)	—	—	—	—	1580	1.67	Oil	1st: 1148 2nd: 1148	2.5 2.5	Polymer Polymer
	H2-7	3-in. nut	—	—	—	1580	1.5	Oil	1148	2.33	Polymer

Table 5—Heat Treatment Details of the Bolts and Nuts Prior to Machining (Phase II)

Bolt Heats	Heat No.	Bolt/ Nut	Normalizing			Austenitizing			Tempering		
			Temp. °F	Time h	Cooling Media	Temp. °F	Time h	Cooling Media	Temp. °F	Time h	Cooling Media
Heat 1	H1-1	1-in. bolt	1650	3.0	Air	1600	3.0	Oil	1155	3.0	Water
	H1-2	1-in. nut	1650	2.5	Air	1575	2.5	Polymer	1155	2.5	Water
	H1-3	3-in. bolt	1650	3.5	Air	1575	3.5	Oil	1st: 1166 2nd: 1115	3.5 3.5	Water Water
	H1-4	3-in. nut	1650	3.5	Air	1600	3.5	Oil	1155	3.5	Water
Heat 2	H2-1	1-in. bolt	—	—	—	1580	1.5	Oil	1148	3.5	Polymer
	H2-2	1-in. nut	—	—	—	1580	1.67	Oil	1148	2.33	Polymer
	H2-3	3-in. bolt	—	—	—	1580	2.0	Oil	1st: 1148 2nd: 1148	2.33 3.0	Polymer Polymer
	H2-4	3-in. nut	—	—	—	1580	1.67	Oil	1148	2.33	Polymer

5.1.5 Mechanical Properties

Mechanical properties, including yield strength at 0.2 % offset line, ultimate tensile strength (UTS), percent elongation, percent reduction in area (RA), hardness in Rockwell C scale, and Charpy V-Notch impact value at –75 °F (Heat 1) and –150 °F (Heat 2) for Phase I and Phase II, are given in Tables 6 and 7, respectively.

NOTE The bolting actual yield strength was limited to a maximum value of 120 ksi (828 MPa).

Table 6—Mechanical Properties of the Bolts and Nuts (Phase I)

Bolt Heats	Heat No.	Bolt/ Nut	Yield Strength, ksi	UTS, ksi	Elongation, %	RA, %	Hardness HRC or (HB)	CVN Impact Value
Manufacturer 1	H1-1	1-in. bolt	116.7	133.3	23.5	63	28–28	88, 82, 82 ft-lbs at –75 °F
	H1-2 (31 off)	1-in. nut	—	—	—	—	28–31	74, 74, 76 ft-lbs at –75 °F
	H1-3 (10 off)	1-in. nut	—	—	—	—	27–30	74, 74, 72 ft-lbs at –75 °F
	H1-4	2-in. bolt	117.4	135.0	23	63.2	28–29	62, 66, 77 ft-lbs at –75 °F
	H1-5	2-in. nut	—	—	—	—	28–30	79, 76, 77 ft-lbs at –75 °F
	H1-6	3-in. bolt	120.9	138.7	24.0	63.2	29–30	76, 80, 80 ft-lbs at –75 °F
	H1-7	3-in. nut	—	—	—	—	30–32	32, 46, 33 ft-lbs at –75 °F
Manufacturer 2	H2-1	1-in. bolt	113.8	130.7	22.4	62.1	28–29 (272–279)	33, 26, 31 ft-lbs at –150 °F
	H2-2	1-in. nut	—	—	—	—	29–30 (281–294)	26.5, 28, 29.5 ft-lbs at –150 °F
	H2-3	2-in. bolt	105.9	128.9	24.0	63.1	28–29 (273–294)	21.4, 20.7, 20.7 ft-lbs at –150 °F
	H2-4	2-in. nut	—	—	—	—	29–29 (278–293)	34.7, 33.2 29.5 ft-lbs at –150 °F
	H2-5 (11 off)	3-in. bolt	113.9	132.3	25.0	62.3	28–28 (283–291)	31, 31, 32.5 ft-lbs at –150 °F
	H2-6 (12 off)	3-in. bolt	115.3	133.5	24.4	63.4	28–29 (278–293)	26.6, 25.8 28.8 ft-lbs at –150 °F
	H2-7	3-in. nut	—	—	—	—	26–26 (278–297)	21.4, 26.5, 28.03 ft-lbs at –150 °F

Table 7—Mechanical Properties of the Bolts and Nuts (Phase II)

Bolt Heats	Heat No.	Bolt/ Nut	Yield Strength, ksi	UTS, ksi	Elongation, %	RA, %	Hardness HRC or (HBW)	CVN Impact Value
Manufacturer 1	H1-1	1-in. bolt	115	133.7	24.5	64	29–31	75, 76, 84 ft-lbs at –75 °F
	H1-2	1-in. nut	—	—	—	—	30–32	36, 42, 36 ft-lbs at –75 °F
	H1-3	3-in. bolt	114.3	133.3	23.4	65	29–31	69, 67, 68 ft-lbs at –75 °F
	H1-4	3-in. nut	—	—	—	—	29–30	76, 77, 77 ft-lbs at –75 °F
Manufacturer 2	H2-1	1-in. bolt	115.7	129.5	22	58.9	28–29	36, 40, 41 ft-lbs at –150 °F 81, 73, 88 ft-lbs at –75 °F
	H2-2	1-in. nut	—	—	—	—	26–27 (258–264)	45, 43, 46 ft-lbs at –150 °F 80, 82, 81 ft-lbs at –75 °F
	H2-3	3-in. bolt	113.9	132.7	22.9	62.0	29–30	35, 35, 38 ft-lbs at –150 °F 74, 69, 74 ft-lbs at –75 °F
	H2-4	3-in. nut	—	—	—	—	2627 (264)	33, 34, 38 ft-lbs at –150 °F 79, 83, 83 ft-lbs at –75 °F

5.2 S-N Fatigue Testing

5.2.1 General

Full-scale fatigue testing programs of low-alloy steel bolts were conducted for bolt sizes of 1 in., 2 in., and 3 in. in Phase I and for bolt sizes of 1 in. and 3 in. in Phase II. Bolts and nuts for each size (diameter) were from two different heats and manufacturers. To develop S-N fatigue curves, the bolts were fatigue tested at three different load levels within the specified load range provided in Tables 8 and 9 for Phase I and Phase II, respectively. Each bolt size was threaded in accordance with ASME B1.1, Class 2 or 3, with 1-in. 8UNCR, 2-in. 8UNR, and 3-in. 8UNR threads, respectively. The stress ranges are based on the root diameter of the threads for each bolt size. Three alternating load/stress levels were applied to each bolt tested. These load/stress levels were defined as: low-stress range fatigue cycles (LFC), medium-stress range fatigue cycles (MFC), and high-stress range fatigue cycles (HFC). Each alternating load/stress level is defined in Tables 8 and 9 for Phase I and Phase II, respectively.

Table 8—Load Levels Applied to Bolts (SMYS = 105 ksi [725 MPa]) (Phase I)

Stress Range Designation	Minimum Axial Stress			Maximum Axial Stress		
	% SMYS	ksi	MPa	% SMYS	ksi	MPa
LFC	67	70	485	75	79	544
MFC	67	70	485	83	87	602
(MFC + 10 %)[a]	67	70	485	91	95	627
HFC	67	70	485	100	105	725

[a] 10 % increase in maximum load.

Table 9—Load Levels Applied to Bolts (SMYS = 105 ksi [725 MPa]) (Phase II)

Stress Range Designation	Minimum Stress			Maximum Stress		
	% SMYS	ksi	MPa	% SMYS	ksi	MPa
HFC	50	52.5	362	100	105	725
MFC	50	52.5	362	83	87.2	602
LFC	50	52.5	362	67	70.4	486

[a] 10 % increase in maximum load.

Table 10 shows the bolt dimensions and the calculated nominal root diameter and corresponding nominal root area for each bolt size.

Table 10—Bolt Dimensions and Calculated Nominal Root Area for Each Bolt Size

Bolt Diameter		Bolt Length		Class 2A Nominal Root Diameter		Nominal Root Area	
in.	cm	in.	cm	in.	cm	$in.^2$	cm^2
1	2.54	7	17.8	0.8390	2.131	0.5528	3.566
2	5.08	18	45.7	1.8382	4.669	2.6538	17.121
3	7.62	28	71.1	2.8376	7.208	6.3239	40.799

Tables 11 and 12 show the stress range designation, stress range corresponding loads, and mean stress that were applied to each bolt size during testing in Phase I and Phase II, respectively, in both ambient air (dry) and SW+CP (wet) environments. The S-N tests in ambient air were conducted to produce reference S-N curves for each bolt size.

Table 11—Applied Stress Ranges and Corresponding Loads for Each Bolt Size (Phase I)

Bolt Diameter		Stress Range Designation	Stress Range, Δσ			Minimum Load		Maximum Load		Mean Stress
in.	cm		ksi	MPa	lbs	kN	lbs	kN	ksi	MPa
1	2.54	HFC	35	241	38,890	173	58,223	259	88	607
		MFC + 10 %	25	174	38,890	173	52,828	215	83	572
		MFC	17	116	38,890	173	48,332	194	79	545
2	5.08	HFC	35	241	186,584	830	278,527	1239	88	607
		MFC	17	116	186,584	830	231,094	928	79	545
		LFC+4 %	11.5	79	186,584	830	217,156	966	76	524
3	7.62	HFC	35	241	445,554	1982	664,958	2958	88	607
		MFC	17	118	445,554	1982	551,884	2455	79	545
		LFC	9	62	445,554	1982	502,428	2235	75	517

Table 12—Applied Stress Ranges and Corresponding Loads for Each Bolt Size (Phase II)

Bolt Diameter		Stress Range Designation	Stress Range, Δσ		Minimum Load		Maximum Load		Mean Stress	
in.	cm		ksi	MPa	lbs	kN	lbs	kN	ksi	MPa
1	2.54	HFC	52.5	362	29,068	129	58,136	259	78.9	544
		MFC	34.7	239	29,068	129	48,244	215	69.9	482
		LFC + 10 % [a]	24.9	172	29,068	129	42,849	191	65	448
		LFC + 7.5 % [b]	22.8	157	29,068	129	41,702	186	64	441
		LFC + 5 % [c]	21.5	148	29,068	129	40,960	182	63.3	436
3	7.62	HFC	52.5	362	332,494	1479	664,988	2958	78.9	544
		MFC	34.7	239	332,494	1479	551,909	2455	69.9	482
		LFC	17.9	123	332,494	1479	445,573	1982	61.5	424

[a] 10 % increase in maximum load.
[b] 7.5 % increase in maximum load.
[c] 5 % increase in maximum load.

5.2.2 S-N Fatigue Testing in an Ambient Air (Dry) Environment

5.2.2.1 Phase I

Prior to S-N testing and after any major changes to the test frames/test equipment, the alignment of the test frames (machines) was verified in accordance with ISO 23788:2012 [10]. To expedite the testing, two load frames (MTS 1000 kN and Instron 300 kN) [1] were used to test the 1-in. bolts. The 2-in. and 3-in. bolts were tested using an Instron 4000 kN load frame.

The test frequency for 1-in. bolt size was 10 Hz and for 2-in. and 3-in. bolt sizes was between 1.5 Hz and 3 Hz. For all bolt sizes, the maximum/minimum applied loads and displacements at the specific applied stress range were recorded and saved for post-test review.

The stress range designation for all bolt sizes in air are shown in Table 11. The stress range designations of MFC + 10 % (which indicates 10 % increase in maximum load) for 1-in. bolts and LFC + 4 % (which indicates 4 % increase in maximum load) for 2-in. bolts were defined and applied to avoid runout. This is because 1-in. bolts at MFC and 2-in. bolts at LFC exhibited runout.

---

1 "MTS 1000 kN" and "Instron 300 kN" are used as examples only and do not constitute an endorsement of any specific product or company by API.

5.2.2.2 Phase II

Prior to S-N testing and after any major changes to the test frames/test equipment, the alignment of the test frames (machines) was verified in accordance with ISO 23788:2012. A 500 kN load frame was used for in-air (dry) testing of 1-in. bolts, and the experiments were conducted at 5 Hz loading frequency. For testing of the 3-in. bolts, a 4000 kN test machine and a loading frequency of 0.3 Hz was used. For both bolt sizes, the maximum/minimum applied loads and displacements at the specific applied stress range were recorded and saved for post-test review.

The stress range designations for both bolt sizes are shown in Table 12. 1-in. bolts at LFC exhibited infinite lives (runout). Therefore, the maximum load increased 10 %, 7.5 %, and finally 5 % to obtain finite lives or to avoid runouts.

5.2.3 S-N Fatigue Testing in an SW+CP (Wet) Environment

For SW+CP testing, the same load frames were used for each specific bolt size. Each load frame was again subjected to a complete and thorough load frame alignment and calibration procedure as in the ambient air tests.

The SW test solution consisted of 3.5 wt. % sodium chloride (NaCl) in deionized water. The purpose of using deionized water was to avoid precipitation of calcareous scale on the surface of the bolts during testing, which can reduce hydrogen uptake during CP. The target solution pH of 8.2 was achieved and kept constant with the addition of either NaOH/NaCl solution of pH = 12 or HCl/NaCl solution of pH = 2. The SW oxygen concentration was reduced and maintained at less than 20 ppb during each test. The SW temperature in the test chamber was controlled and maintained at 39.2 °F (4 °C).

Prior to cyclic loading, each bolt was pre-charged at an applied potential of –1050 mV versus saturated calomel electrode (SCE) for four days under the defined preload, and the applied potential was maintained until termination of the test. After the pre-charging period, the alternating stress given in Table 11 and Table 12 was applied to each bolt at the frequency of 0.3 Hz until the bolt failure.

For each bolt tested in SW+CP, the following data were recorded:

— test solution temperature in the test chamber;

— maximum/minimum load, as well as maximum/minimum displacement;

— oxygen concentration;

— solution pH;

— applied CP potential;

— number of cycles to failure.

5.2.4 S-N Fatigue Testing in Air and SW+CP Environments (Phase I)

5.2.4.1 General

Tables 13 to 18 show the S-N test results for the 1-in., 2-in. and 3-in. bolts, respectively. For each bolt size from each heat, the defined plan was to perform three S-N tests at HFC (H), three at MFC (M), and three at LFC (L). The bolting exhibited better-than-expected life and therefore, with the limited and defined total cycles allocated for the test program, the original test plan was not met, lacking information for some of the bolt sizes and stress ranges.

Table 13—S-N Fatigue Test Results for 1-in. Bolts in Air (Phase I)

Specimen ID	Heat	Stress Range, Δσ		Cycles to Failure	Comments
		ksi	MPa		
1-D-H-U-1	1	35	241	46,373	—
1-D-H-U-2	1	35	241	46,788	—
1-D-M-U-3	1	17	118	3,249,584	runout
1-D-M-U-3–2	1	25	174	139,104	MFC + 10 %
1-D-M-U-4	1	25	174	141,828	MFC + 10 %
1-D-H-U-5	1	35	241	44,212	—
1-D-M-U-6	1	17	118	3,590,920	runout
1-D-M-U-6–2	1	25	174	202,464	MFC + 10 %
1-D-M-U-7	1	17	118	717,557	—
1-D-M-U-8	1	17	118	24,181,373	runout
1-D-H-O-1	2	35	241	60,415	—
1-D-H-O-2	2	35	241	68,082	—
1-D-H-O-3	2	35	241	49,611	—
1-D-M-O-4	2	17	118	2,493,418	runout
1-D-M-O-4–2	2	25	174	29,4771	MFC + 10 %
1-D-M-O-5	2	17	118	703,439	—
1-D-M-O-6	2	17	118	12,933,856	runout
1-D-M-O-7	2	17	118	1,141,077	—

Table 14—S-N Fatigue Test Results for 1-in. Bolts in an SW+CP Environment (Phase I)

Specimen ID	Heat	Stress Range, Δσ		Cycles to Failure	Comments
		ksi	MPa		
1-W-H-U-1	1	35	241	22,699	—
1-W-H-U-2	1	35	241	21,144	—
1-W-H-U-3	1	25	241	19,981	—
1-W-M-U-4	1	25	174	41,875	MFC + 10 %
1-W-M-U-5	1	17	174	36,311	MFC + 10 %
1-W-M-U-6	1	17	118	149,290	—
1-W-M-U-7	1	17	118	147,983	—
1-W-M-U-8	1	17	118	133,662	—
1-W-M-U-9	1	35	118	163,450	—
1-W-H-O-1	2	35	241	19,423	—
1-W-H-O-2	2	35	241	21,147	—
1-W-H-O-3	2	35	241	26,837	—
1-W-M-O-4	2	17	118	189,014	—
1-W-M-O-5	2	17	118	256,895	—
1-W-M-O-6	2	17	118	189,002	—
1-W-M-O-7	2	17	118	158,313	—
1-W-M-O-9	2	17	118	149,135	correct potential
1-W-M-O-10	2	17	118	299,241	correct potential
1-W-M-O-11	2	17	118	180,708	correct potential
1-W-L-O-8	2	9	59	1,635,607	LFCa, runout. Test stopped
1-W-L-O-12	2	12	80	1,260,569	LFCa+4 %, runout. Test stopped

Table 15—S-N Fatigue Test Results for 2-in. Bolts in Air (Phase I)

Specimen ID	Heat	Stress Range, Δσ		Cycles to Failure	Comments
		ksi	MPa		
2-D-H-U-1	1	35	239	33,824	—
2-D-H-U-2	1	35	239	31,852	—
2-D-H-U-3	1	35	239	35,448	—
2-D-M-U-4	1	17	118	299,286	—
2-D-M-U-5	1	17	118	322,676	—
2-D-M-U-6	1	17	118	285,899	—
2-D-L-U-7	1	11.6	80	16,735,547	LFC[a]+4 %, runout. Test stopped
2-D-H-O-1	2	35	239	42,600	—
2-D-H-O-2	2	35	239	41,957	—
2-D-H-O-3	2	35	239	40 975	—
2-D-M-O-4	2	17	118	353,630	—
2-D-M-O-5	2	17	118	352,474	—
2-D-M-O-6	2	17	118	257,321	—

Table 16—S-N Fatigue Test Results for 2-in. Bolts in an SW+CP Environment (Phase I)

Specimen ID	Heat	Stress Range, Δσ		Cycles to Failure	Comments
		ksi	MPa		
2-W-H-U-1	1	35	239	22,753	—
2-W-H-U-2	1	35	239	24,290	—
2-W-H-U-3	1	35	239	25,807	—
2-W-M-U-4	1	17	118	123,493	—
2-W-H-O-1	2	35	239	28,133	—
2-W-H-O-2	2	35	239	26,871	—
2-W-H-O-3	2	35	239	27,206	—

Table 17—S-N Fatigue Test Results for 3-in. Bolts in Air (Phase I)

Specimen ID	Heat	Stress Range, Δσ		Cycles to Failure	Comments
		ksi	MPa		
3-D-H-U-1	1	35	239	28,931	—
3-D-H-U-2	1	35	239	28,990	—
3-D-H-U-3	1	35	239	28,968	—
3-D-M-U-4	1	17	118	245,237	—
3-D-M-U-5	1	17	118	327 091	—
3-D-M-U-6	1	17	118	238 083	—
3-D-M-U-7	1	8.4	58	10,482,717	LFC, runout
3-D-H-O-1	2	35	239	30,095	—
3-D-H-O-2	2	35	239	29,989	—
3-D-H-O-3	2	35	239	30,254	—
3-D-M-O-4	2	17	118	199,318	—
3-D-M-O-5	2	17	118	223,213	—
3-D-M-O-6	2	17	118	203,548	—
3-D-L-O-7	2	8.4	58	10,883,093	LFC, runout

Table 18—S-N Fatigue Test Results for 3-in. Bolts in an SW+CP Environment (Phase I)

Specimen ID	Heat	Stress Range, Δσ		Cycles to Failure	Comments
		ksi	MPa		
3-W-H-U-1	1	35	239	23,676	—
3-W-M-U-4	1	17	118	116,184	—
3-W-M-U-5	1	17	118	112,301	—
3-W-H-O-1	2	35	239	25,649	—
3-W-H-O-2	2	35	239	24,395	—
3-W-H-O-3	2	35	239	25,516	—
3-W-M-O-4	2	17	118	115,689	—
3-W-M-O-5	2	17	118	128,350	—

A couple samples (1-D-M-O-5 and 1-D-M-U-7) tested at MFC in air exhibited lower fatigue life than rest of the samples, which exhibited either runouts or over one million cycles of fatigue life. To assess this large variation in results, an investigation was conducted on the two load frames that were used to test the 1-in. bolts, as well as the thread root profiles of the bolts that showed different fatigue lives.

Thorough investigation of the applied maximum and minimum loads at $\Delta\sigma = 17$ ksi (118 MPa) between the two load frames using dummy test specimens showed that the test result discrepancy for 1-in. bolts in ambient air is not due to the load frames.

Figure 1 shows high-magnification images taken from bolt sample 1-D-M-U-7 (717,557 cycles of fatigue life) and 1-D-M-O-5 (703,439 cycles of fatigue life), respectively. Bolt sample 1-D-M-U-7 (Figure 1a) contains a smoother thread root profile than bolt sample 1-D-M-O-5, which contains a rougher surface (white arrow in Figure 1b). Additionally, the bolt in Figure 1a had a nonuniform loading on the thread flank that appeared to cause an uneven load distribution on the threads (see Figure 2).

The rougher thread root profile in Figure 1b could be due to a worn or dull tool during threading. The surface imperfections of the root profile will act as a stress riser and can reduce the number of cycles to fatigue crack initiation and, hence, total fatigue life of the bolts. The scanning electron microscopy (SEM) image in Figure 1c clearly shows fatigue crack initiation from the surface imperfections on the thread root, which can result in a finite life at the applied stress range of $\Delta\sigma = 17$ ksi (118 MPa).

Further investigation of bolt sample 1-D-M-U-7 with smooth thread root profiles showed that the bolt contained an imperfection (e.g., potentially due to machining) that went all the way around the first thread flank, as shown in Figure 2. Even with a smooth thread root profile, such imperfections on the thread flanks will act as stress risers and can reduce the number of cycles for crack initiation and, hence, total fatigue life of the bolt.

The metallurgical investigation suggested that the lower fatigue life observed from certain bolt samples such as 1-D-M-O-5 and 1-D-M-U-7 are likely associated with rougher thread surface profiles or imperfections on the thread flank, although all the tested bolts from the two heats were conforming with the requirements of API 20E BSL-3.

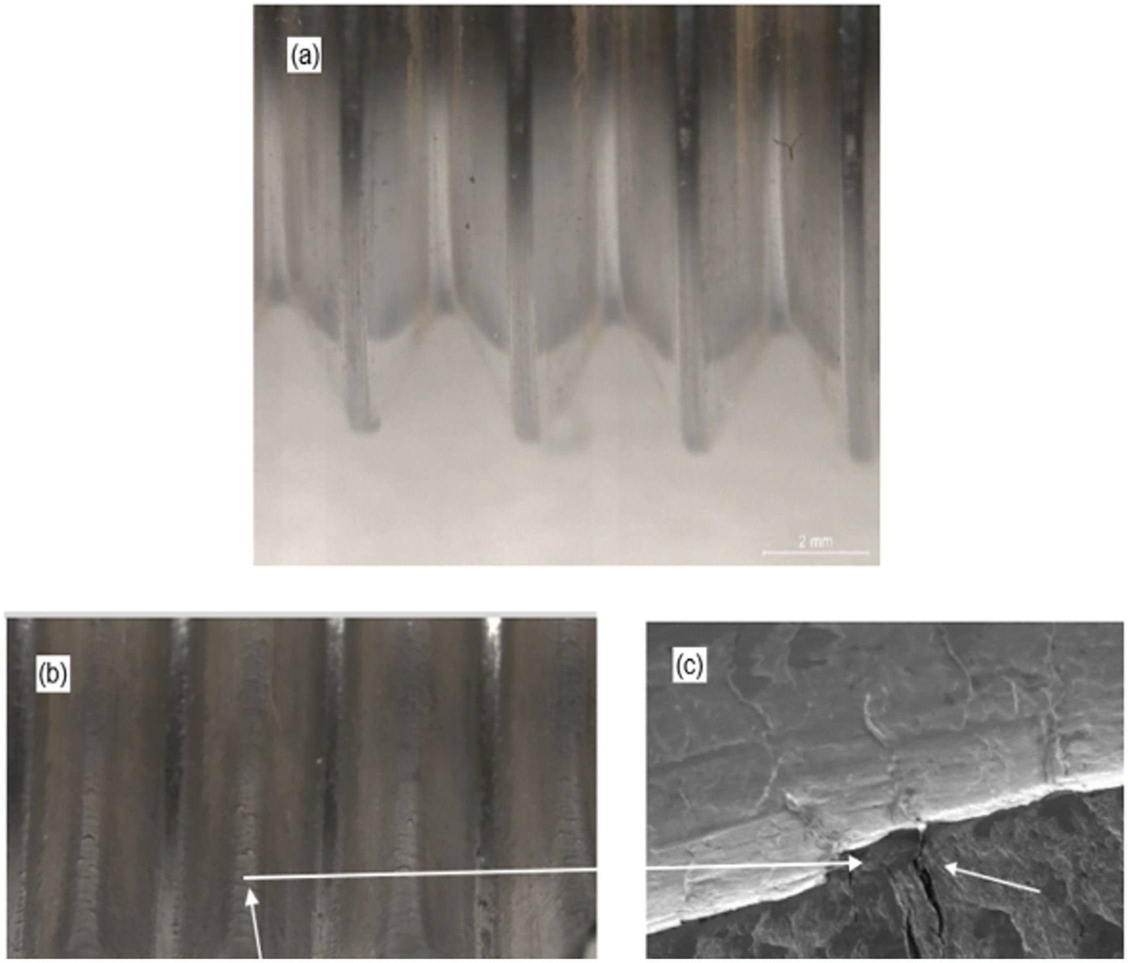

Key

(a) Thread profile of Sample 1-D-M-U-7 indicating a smoother surface roughness.

(b) Rougher surface roughness (white arrow) of Sample 1-D-M-O-5 perhaps due to dull machine tool.

(c) SEM image illustrating crack initiation (white arrow) from the rougher thread root.

Figure 1—Thread Root Profiles

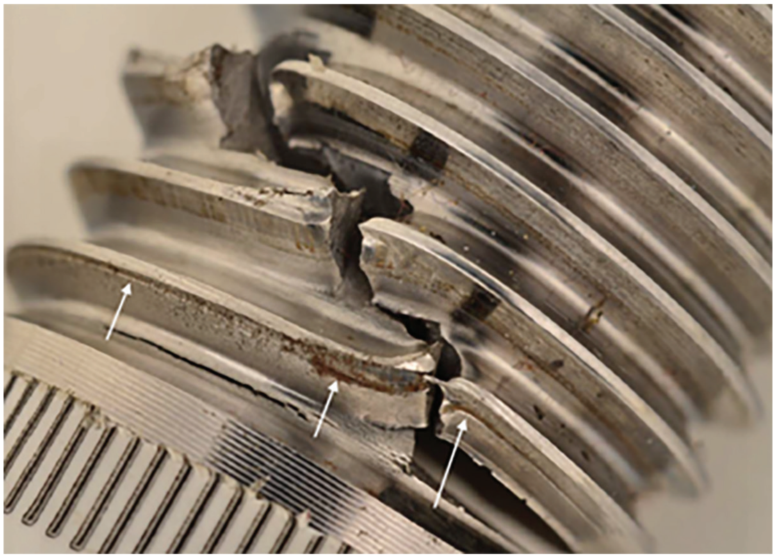

Figure 2—1-in. Bolt, 1-D-M-U-7, Showing an Imperfection in the Thread Flank (White Arrows)

5.2.4.2 Applied Cathodic Potential Effects

Midway through testing of 1-in. bolts in an SW+CP environment, it was realized that the tested bolts were exposed to a more negative potential (–1095 mV versus SCE) instead of –1050 mV versus SCE. The higher negative applied potential was due to using an SCE reference electrode with a different salt concentration. The higher negative applied potential meant that the already-tested 1-in. bolts could have higher absorbed atomic hydrogen and, hence, higher hydrogen permeation through the bolts, which could have resulted in lower fatigue life.

To check this difference in applied potential and its effect on fatigue lives, three extra 1-in. bolts were tested at the correct applied potential of –1050 mV (versus SCE with the correct salt concentration), as shown in Table 14. All bolts were exposed to a stress range of $\Delta\sigma = 17$ ksi (118 MPa). The results in Table 14 illustrate that at the correct applied potential, the corresponding fatigue lives are in the same range as the bolts exposed to the higher negative potential. This ensured that the initial tests in SW+CP were not adversely affected by the slightly more negative applied potential.

5.2.5 S-N Fatigue Curves in Air and SW+CP Environments (Phase I)

Figure 3, Figure 4, and Figure 5 show the S-N fatigue curves obtained for the 1-in., 2-in., and 3-in. bolts in air, respectively. The plots also show the mean and mean $-t_p$ * standard deviation (SD). The statistical analysis was performed in accordance with the requirements of ASTM E739[11]. One of the requirements of ASTM E739 is that only data points with finite life can be used for statistical analysis. The figures also contain the regression analysis data for each bolt size below each plot. The regression analysis was conducted for the S-N curve with the following power law equation:

$$N = a(\Delta\sigma)^{-m} \tag{1}$$

or

$$\log N = \log a - m\log\Delta\sigma \tag{2}$$

where

N	is the number of cycles to failure;
a	is the intercept of design S-N curve with the log N axis;
m	is the negative inverse slope of the S-N curve;
$\Delta\sigma$	is the stress range.

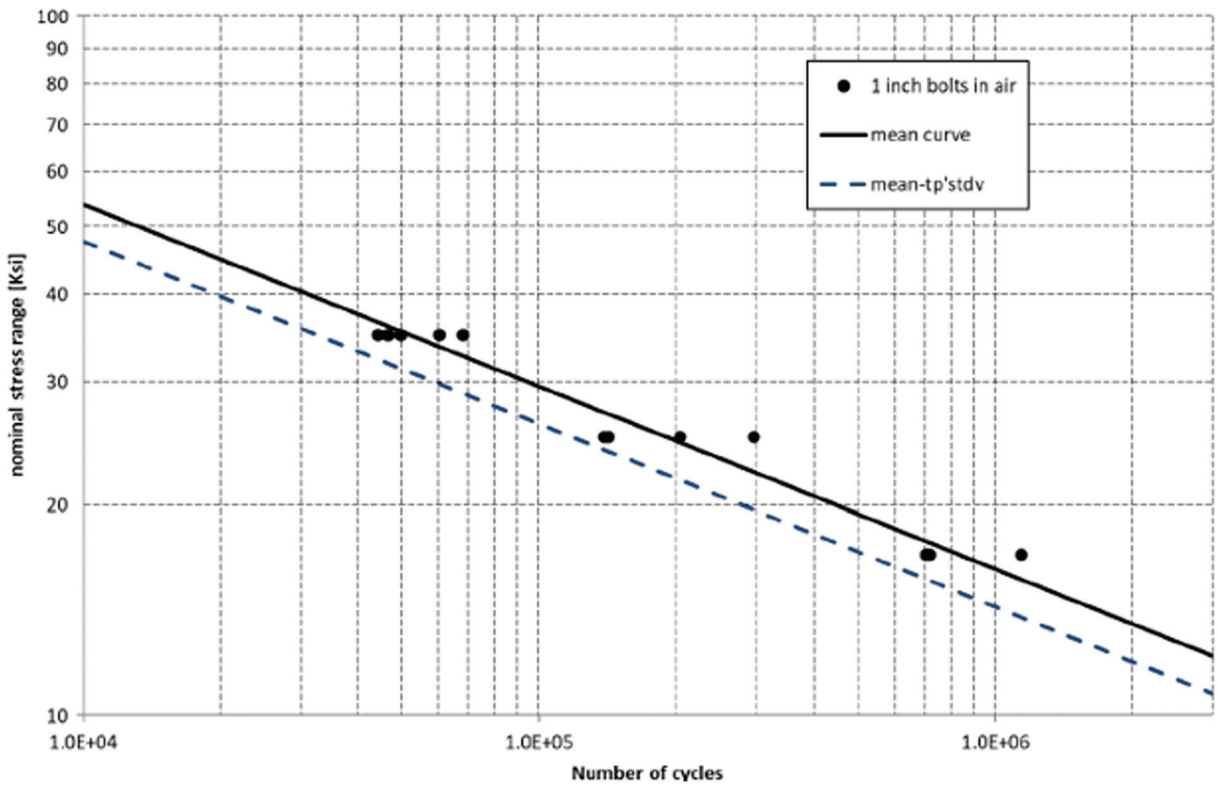

1 in. Air Data	ASTM (ksi)
m =	3.84
$\log a_1$ (mean)	10.637
StD ($\log \overline{a_1}$)	0.103
Tp (13 test data)	2.201
Mean-tp*stdv	10.410

Figure 3—S-N Fatigue Curve for 1-in. Bolts in Air (Phase I)

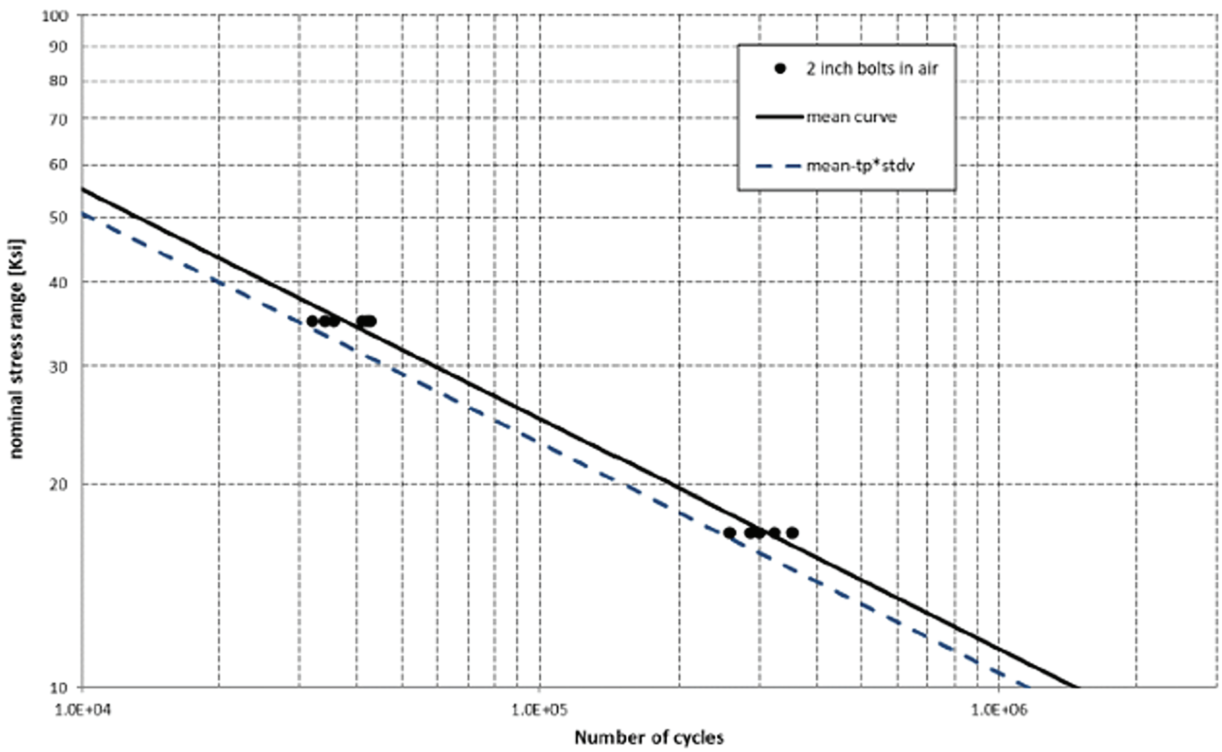

2 in. Air Data	ASTM (ksi)
m =	2.923
$\log a_1$ (mean)	9.088
StD $(\log \overline{a_1})$	0.052
Tp (12 test data)	2.228
Mean-tp*stdv	8.973

Figure 4—S-N Fatigue Curve for 2-in. Bolts in Air (Phase I)

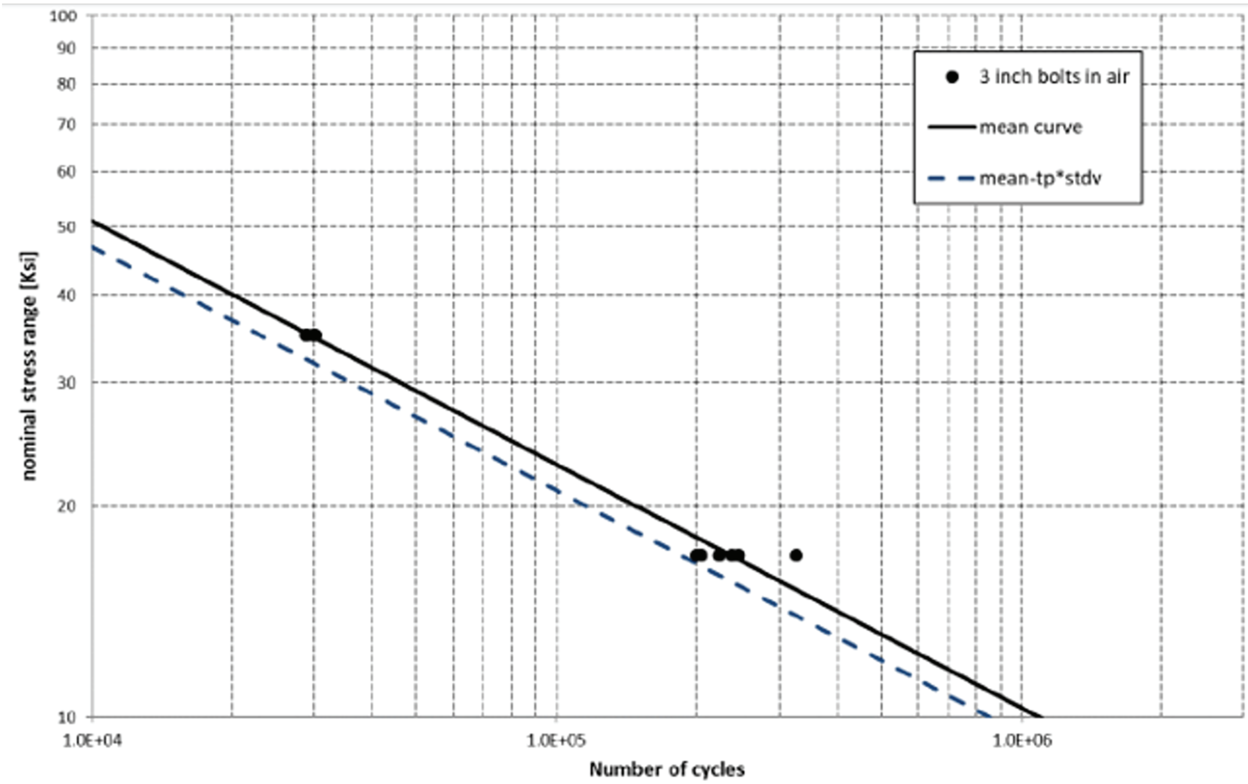

3 in. Air Data	ASTM (ksi)
m =	2.878
$\log a_1$ (mean)	8.915
StD ($\log \overline{a_1}$)	0.053
Tp (12 test data)	2.228
Mean-tp*stdv	8.796

Figure 5—S-N Fatigue Curve for 3-in. Bolts in Air (Phase I)

NOTE The test data for 2-in. and 3 in.-bolts in air at LFC is incomplete. Additional testing at LFC is required to develop the more-accurate design curves.

Figure 6, Figure 7, and Figure 8 show and compare the S-N fatigue curves obtained for the 1-in., 2-in., and 3-in. bolts in air and SW+CP, respectively. The plots also show the mean and mean $-t_p$ * SD in both environments. The statistical analysis for the curves in SW+CP were also performed in accordance with requirements of ASTM E739. The figures also contain the regression analysis data for each bolt size in SW+CP at the bottom of each plot.

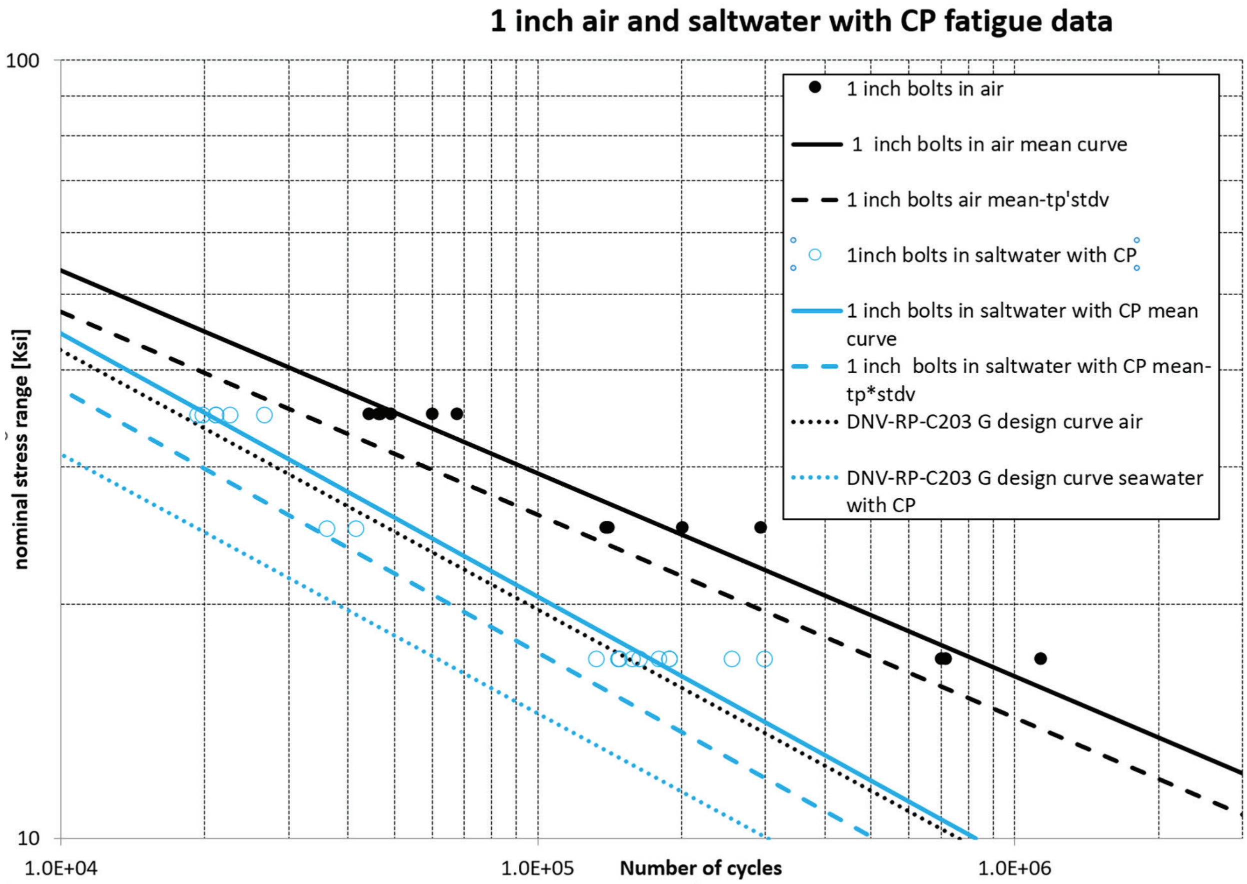

1 in. Saltwater with CP	ASTM (ksi)
m =	2.956
log a_1 (mean)	8.874
StD (log $\overline{a_1}$)	0.101
Tp (13 test data)	2.110
Mean-tp*stdv	8.662

Figure 6—S-N Fatigue Curves for 1-in. Bolts in Air and SW+CP (Phase I)

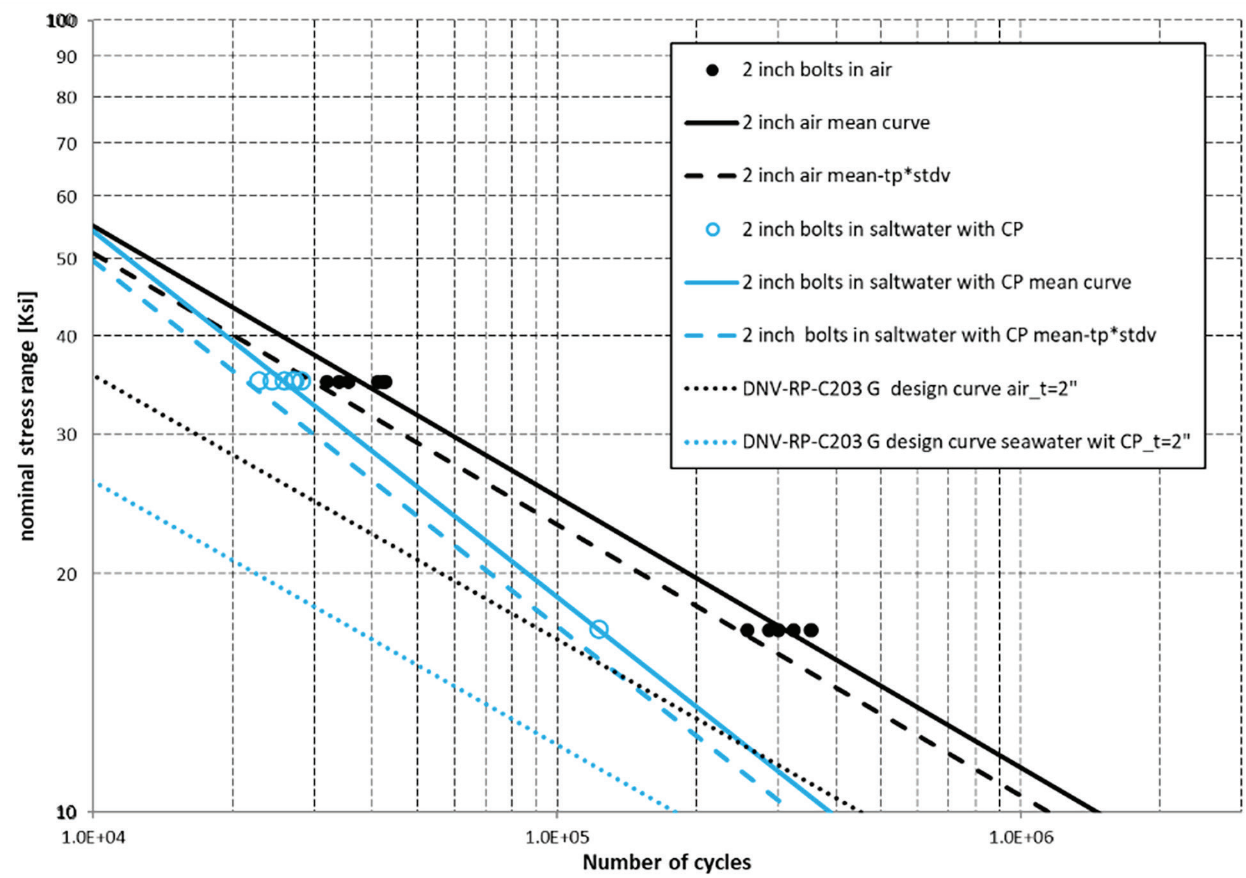

2 in. Saltwater with CP Data	ASTM (ksi)
m =	2.170
$\log a_1$ (mean)	7.761
StD ($\log \overline{a_1}$)	0.031
Tp (7 test data)	2.571
Mean-tp*stdv	7.680

Figure 7—S-N Fatigue Curves for 2-in. Bolts in Air and SW+CP (Phase I)

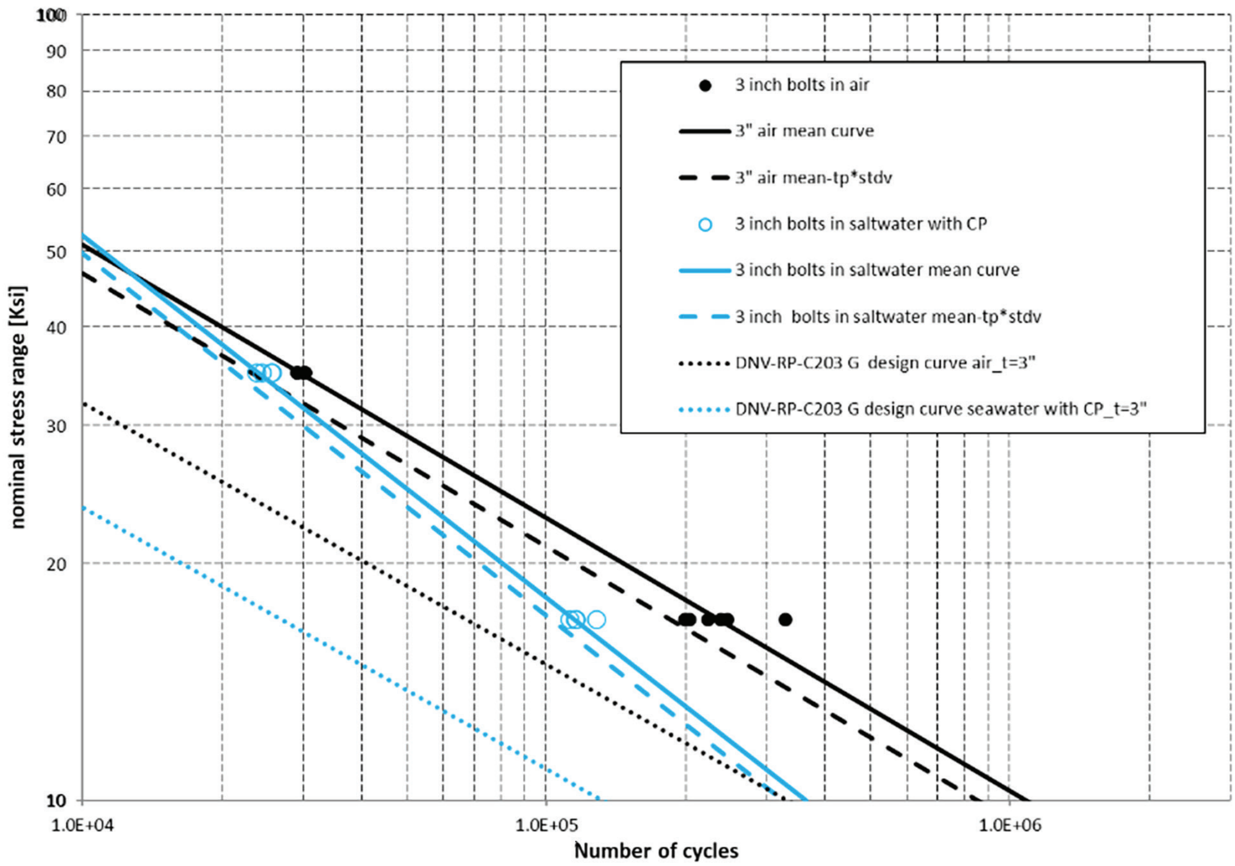

3 in. Saltwater with CP Data	ASTM (ksi)
m =	2.160
$\log a_1$ (mean)	7.730
StD ($\log \overline{a_1}$)	0.020
Tp (8 test data)	2.447
Mean-tp*stdv	7.681

Figure 8—S-N Fatigue Curves for 3-in. Bolts in Air and SW+CP (Phase I)

The data illustrated in these figures shows that at HFC and for all bolt sizes, the fatigue lives in SW+CP and in air are close, while at lower-stress ranges and for all bolt sizes, the fatigue lives in SW+CP are lower than the lives in ambient air, resulting in steeper S-N curves. Also, the larger the bolt diameter, the closer the fatigue lives in SW+CP are to the air values at high-stress ranges.

The results illustrate that at HFC, fatigue lives in SW+CP and in air are more influenced by the root radius stress concentration factor. At LFC, fatigue lives in SW+CP are more influenced by the atomic hydrogen adsorption and diffusion to the fracture process zone beneath the surface at the root radius of the bolt, resulting in lower cycles to crack initiation and, hence, lower overall fatigue life as compared with air.

Based on the developed S-N fatigue curves for 1-in., 2-in., and 3-in. bolts in air and SW+CP environments, Table 19 provides a “knock-down” factor for different stress levels for different bolt sizes.

Table 19—Fatigue Test Knock-down Factors for SW+CP/Air (Phase I)

Stress Range $\Delta\sigma$		1 in.	2 in.	3 in.
ksi	MPa			
35	241	0.42	0.68	0.85
25	174	0.20	—	—
17	118	0.21	0.40	0.50

5.2.6 Post S-N Fatigue Test Evaluation (Phase I)

5.2.6.1 General

Upon completion of each S-N test, the bolts were evaluated, and pictures of their fracture surfaces were taken and documented on a result sheet along with other information specific to each bolt. A few fractured bolts from each heat were selected to be studied further.

5.2.6.2 Hardness Measurements

Three (3) bolts from each size (in total, 6 bolts) were selected to be evaluated. These bolts are 1-W-L-O-9, 1-W-M-U-6, 1-W-M-O-5, 3-W-L-O-8, 3-W-L-U-7, and 3-W-L-U-9. All the selected bolts for post-test hardness evaluation were S-N fatigue tested in an SW+CP environment. The purpose was to determine if any work/strain hardening took place due to the stresses at the first and second engaged threads, as well as hydrogen concentration at these locations. Vickers hardness (HV1 and HV10) scale was used, and the measured values were converted to Rockwell C scale per ASTM E140 [12]. Figure 9 shows schematically the location of the hardness measurement. Tables 20 to 25 provide the measured Vickers hardness and the corresponding converted Rockwell C values.

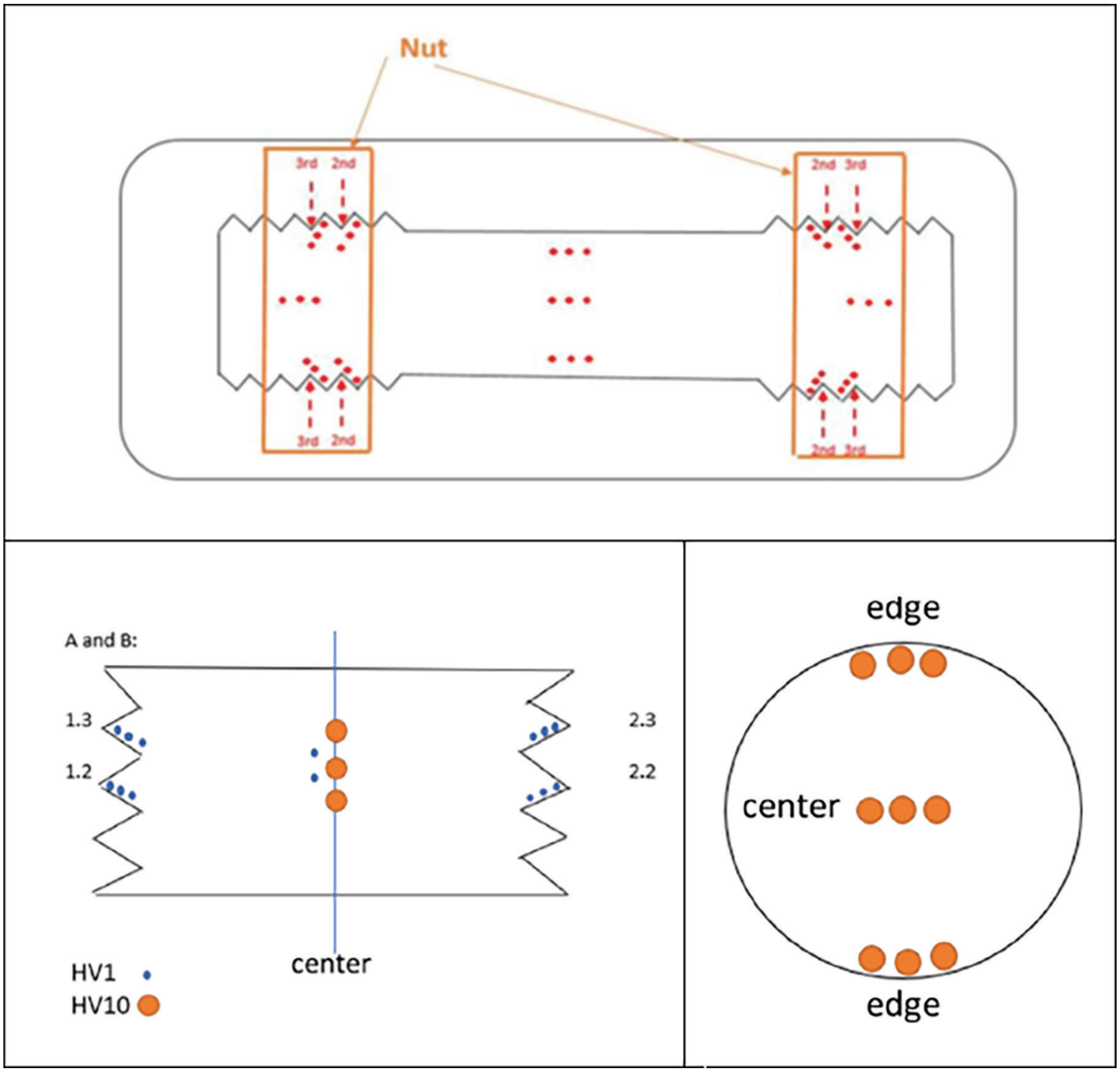

Figure 9—Schematics of Vickers Hardness Test Locations

Table 20—Hardness Measurement Results for 1-in. Bolt from Heat 1 (Phase I)

Hardness Reading Location	A		B		C		
	HV1	HRC	HV1	HRC	Hardness Test Location	HV10	HRC
1.2	282	27	273	28	Edge 1	286	28
	282	27	282	26		284	28
	276	26	289	27		288	28
1.3	276	26	283	28	Edge 2	292	29
	280	27	283	27		291	29
	291	29	288	27		291	29
2.2	288	28	280	28	Center	280	27
	291	29	272	27		282	27
	280	27	289	26		283	27
2.3	289	28	286	28	—	—	—
	291	29	269	28	—	—	—
	292	29	285	25	—	—	—
Center (HV1)	280	27	285	28	—	—	—
	282	27	285	28	—	—	—
	282	27	284	28	—	—	—
Center (HV10)	283	27	278	27	—	—	—
	282	27	277	27	—	—	—
	282	27	280	27	—	—	—

Table 21—Hardness Measurement Results for 1-in. Bolt from Heat 2 (Phase I)

Hardness Reading Location	A		B		C		
	HV1	HRC	HV1	HRC	Hardness Test Location	HV10	HRC
1.2	298	29	297	29	Edge 1	293	29
	297	29	298	29		293	29
	291	29	294	29		295	29
1.3	305	30	292	29	Edge 2	295	29
	298	29	297	29		299	30
	298	29	293	29		300	30
2.2	300	30	304	30	Center	295	29
	307	31	291	29		297	29
	304	30	303	30		300	30
2.3	297	29	289	28	—	—	—
	292	29	301	30	—	—	—
	286	28	289	28	—	—	—
Center (HV1)	276	26	293	29	—	—	—
	271	26	290	28	—	—	—
	279	27	301	30	—	—	—
Center (HV10)	276	26	280	27	—	—	—
	282	27	280	27	—	—	—
	286	28	283	27	—	—	—

Table 22—Hardness Measurement Results for 2-in. Bolt from Heat 1 (Phase I)

Hardness Reading Location	A		B		C		
	HV1	HRC	HV1	HRC	Hardness Test Location	HV10	HRC
1.2	304	30	287	28	Edge 1	284	28
	297	29	298	29		273	23
	298	29	285	28		276	26
1.3	303	30	292	29	Edge 2	300	30
	295	29	290	28		302	30
	305	30	293	29		296	29
2.2	295	29	294	29	Center	284	28
	297	29	305	30		273	26
	294	29	291	29		276	26
2.3	282	27	283	27	—	—	—
	285	28	297	29	—	—	—
	296	29	288	28	—	—	—
Center (HV1)	292	29	295	29	—	—	—
	285	28	294	29	—	—	—
	290	28	290	28	—	—	—
Center (HV10)	293	29	284	28	—	—	—
	297	29	292	29	—	—	—
	294	29	287	28	—	—	—

Table 23—Hardness Measurement Results for 2-in. Bolt from Heat 2 (Phase I)

Hardness Reading Location	A		B		C		
	HV1	HRC	HV1	HRC	Hardness Test Location	HV10	HRC
1.2	303	30	291	29	Edge 1	302	30
	304	30	311	31		302	30
	309	31	309	31		305	30
1.3	310	31	306	31	Edge 2	297	29
	314	32	309	31		296	29
	310	31	308	31		298	29
2.2	310	31	313	31	Center	291	29
	313	31	298	29		282	27
	311	31	314	32		275	26
2.3	308	31	310	31	—	—	—
	301	30	313	31	—	—	—
	315	32	318	32	—	—	—
Center (HV1)	300	30	289	28	—	—	—
	294	29	293	29	—	—	—
	307	31	298	29	—	—	—
Center (HV10)	287	28	319	32	—	—	—
	290	28	321	32	—	—	—
	292	29	317	32	—	—	—

Table 24—Hardness Measurement Results for 3-in. Bolt from Heat 1 (Phase I)

Hardness Reading Location	A		B		C		
	HV1	HRC	HV1	HRC	Hardness Test Location	HV10	HRC
1.2	306	31	302	30	Edge 1	299	30
	309	31	304	30		298	29
	315	32	305	30		299	30
1.3	308	31	307	31	Edge 2	300	30
	311	31	309	31		300	30
	310	31	308	31		299	30
2.2	306	30	307	31	Center	293	29
	306	30	315	32		290	28
	302	30	311	31		286	28
2.3	302	30	314	32	—	—	—
	303	30	301	30	—	—	—
	307	31	308	31	—	—	—
Center (HV1)	303	30	299	30	—	—	—
	304	30	305	30	—	—	—
	297	29	313	31	—	—	—
Center (HV10)	290	28	299	30	—	—	—
	289	28	300	30	—	—	—
	291	29	303	30	—	—	—

Table 25—Hardness Measurement Results for 3-in. Bolt from Heat 2 (Phase I)

Hardness Reading Location	A		B		C		
	HV1	HRC	HV1	HRC	Hardness Test Location	HV10	HRC
1.2	288	28	296	29	Edge 1	300	30
	310	31	309	31		295	29
	291	29	302	30		298	29
1.3	304	30	295	29	Edge 2	297	29
	306	31	310	31		297	29
	311	31	311	31		302	30
2.2	292	29	298	29	Center	277	27
	298	29	299	30		275	26
	293	29	294	29		283	27
2.3	304	30	297	29	—	—	—
	292	29	298	29	—	—	—
	305	30	293	29	—	—	—
Center (HV1)	288	28	291	29	—	—	—
	288	28	291	29	—	—	—
	299	30	294	29	—	—	—
Center (HV10)	287	28	290	28	—	—	—
	282	28	291	29	—	—	—
	281	27	293	29	—	—	—

5.2.6.3 Microstructure Examination

Microstructures of the selected bolts from each heat and each size were studied using optical microscopy. The study revealed that all the bolts contained a temper martensite microstructure. Some degree of banding (inhomogeneity in microstructure due to microsegregation in chemical composition) and differences in grain size were observed. This phenomenon can lead to slightly different microstructure after quench and temper. Regions rich in alloying elements yield martensite and bainite microstructures, while the areas with lower alloying elements might yield bainite and ferrite types of microstructures. Microsegregation banding observed is typical of low-alloy steel bolting and is distinctly different than what is prohibited by API 20E.

In this study, 1-in. and 3-in. bolts showed similar quenched and tempered and fine-grained microstructure. Areas of banding mainly at the center of the bolts were visible. The 2-in. bolts from Heat 1 exhibited a more prominent banding than the bolts from Heat 2. Microstructures of examined bolts, at 200X magnification, from Heat 1 and Heat 2 at the thread area and at the center for 1-in. bolts are given in Figure 10.

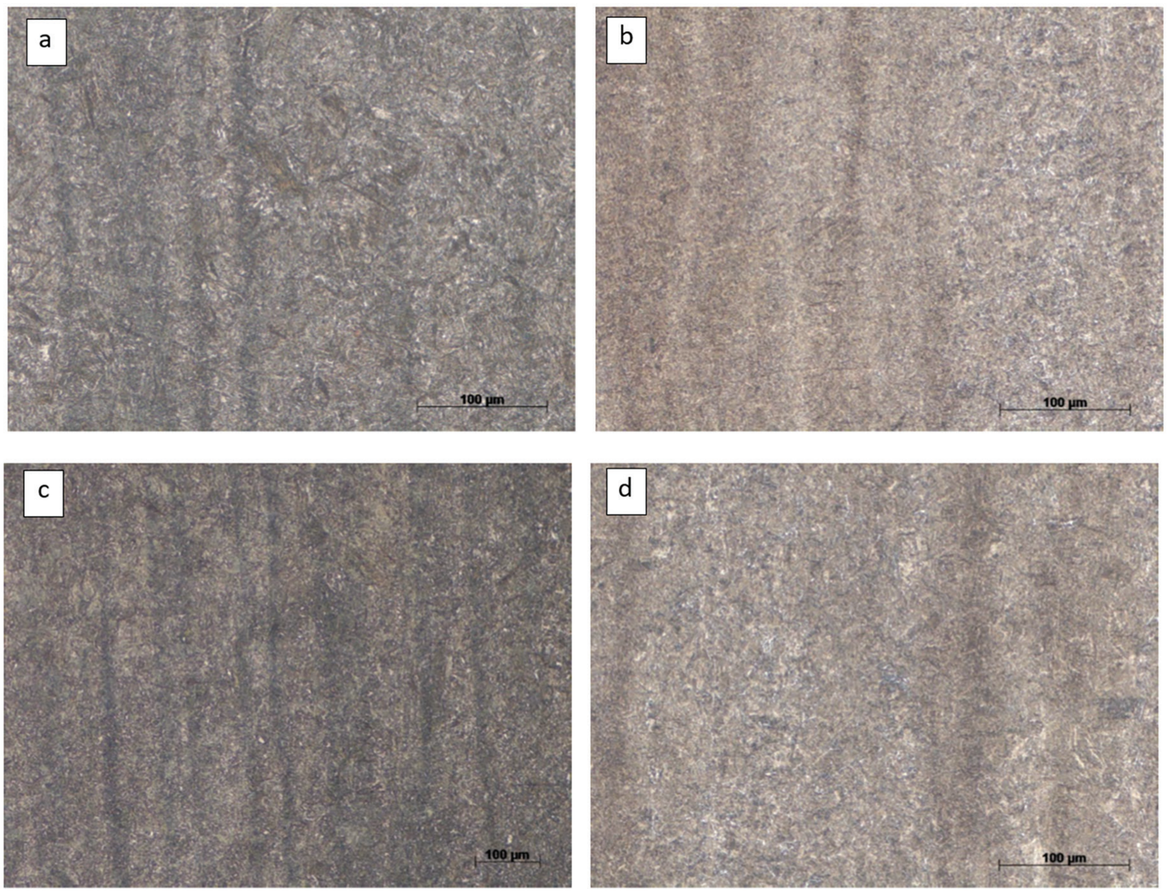

Key
a) at the thread area – Heat 1
b) at the center – Heat 1
c) at the thread area – Heat 2
d) at the center – Heat 2

Figure 10—Optical Microscopy Microstructure of the 1-in. Bolts

Microstructures of examined bolts, at 200X magnification, from Heat 1 and Heat 2 at the thread area and at center for 2-in. bolts are given in Figure 11.

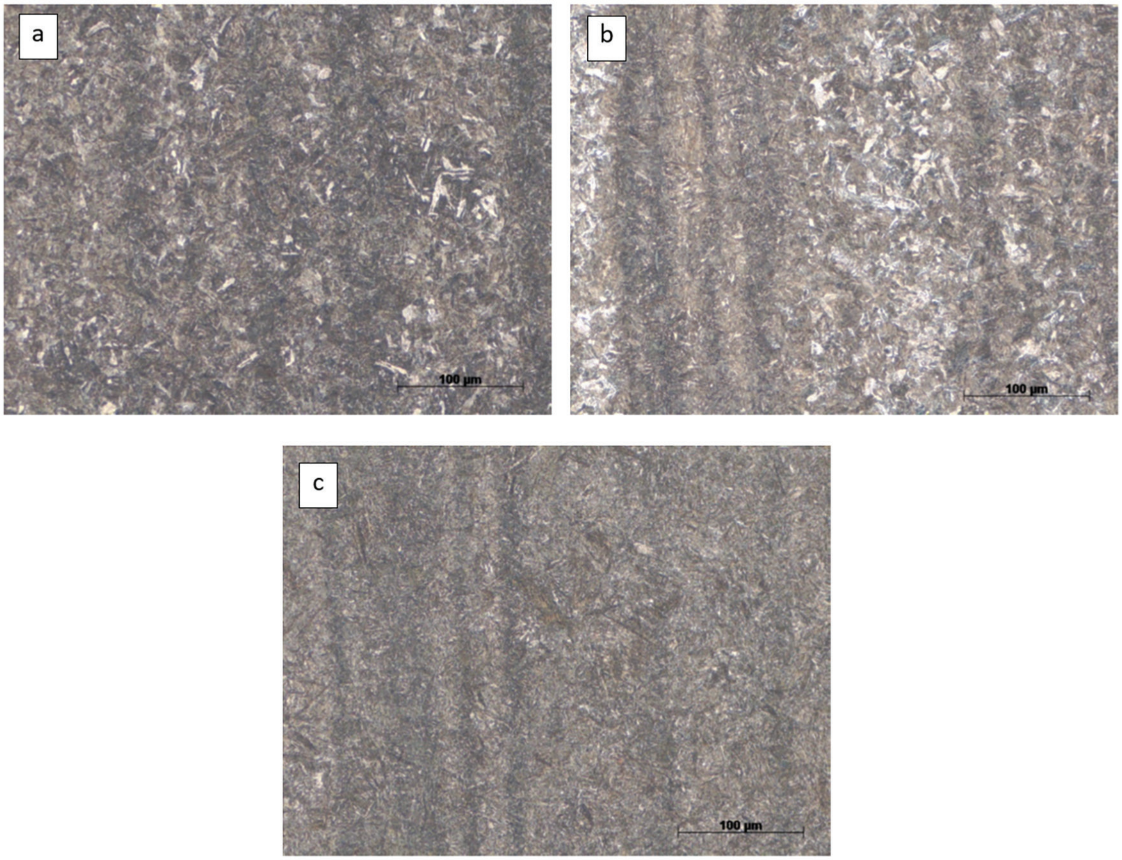

Key
a) at the thread area – Heat 1
b) at the center – Heat 1
c) at the thread area – Heat 2

Figure 11—Optical Microscopy Microstructure of the 2-in. Bolts Magnification 200X (Phase I)

Microstructures of examined bolts, at 200X magnification, from Heat 1 and Heat 2 at the thread area and at the center for 3-in. bolts are given in Figure 12.

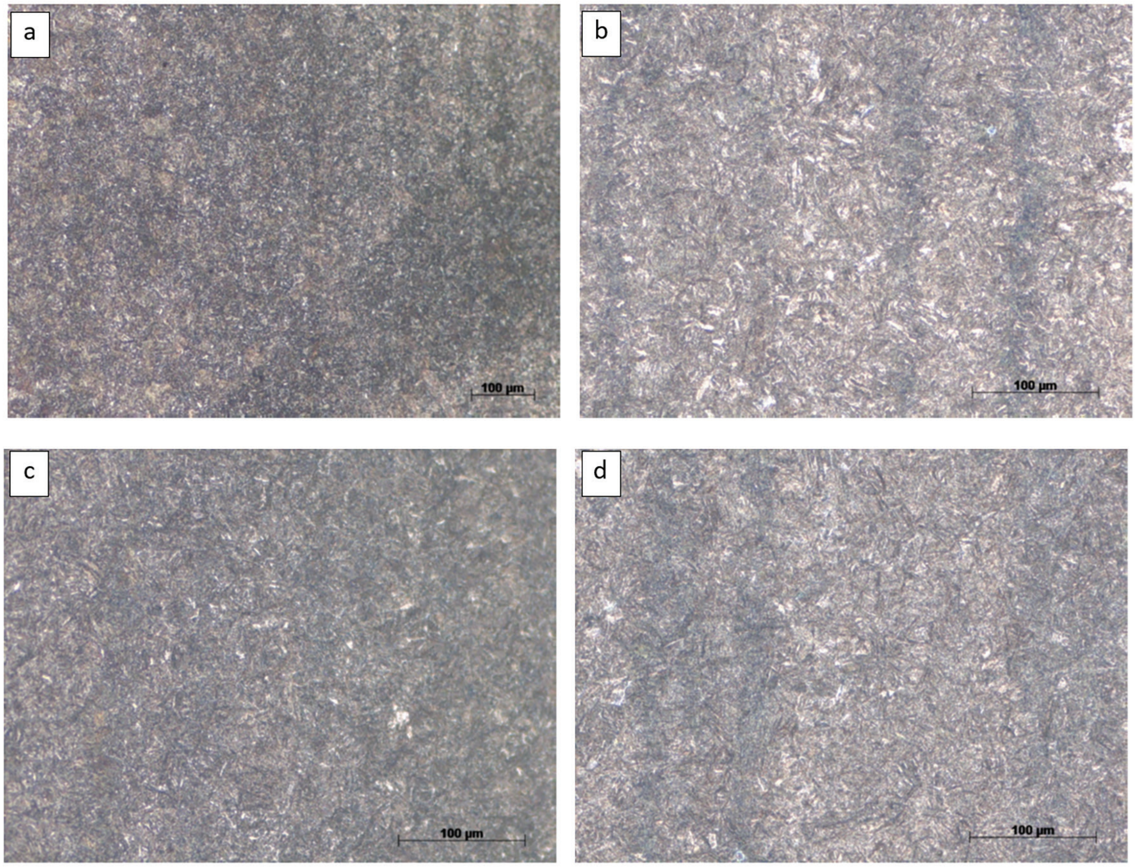

Key
a) at the thread – Heat 1
b) at the center – Heat 1
c) at the thread – Heat 2
d) at the center – Heat 2

Figure 12—Optical Microscopy Microstructure of the 3-in. Bolts Magnification 200X (Phase I)

5.2.7 S-N Fatigue Testing in Air and in SW+CP (Phase II)

S-N testing of the bolts in Phase II was performed with a defined preload of 50 % of SMYS, and the applied stress ranges and corresponding loads for each bolt size are given in Table 12. Tables 26 to 29 show the test results in air and in SW+CP environments for the 1-in. and 3-in. bolts, respectively.

Table 26—S-N Fatigue Test Results for 1-in. Bolts in Air (Phase II)

Specimen ID	Heat	Stress Range, Δσ		Cycles to Failure	Comments
		ksi	MPa		
1-D-H-U-1	1	52.6	363	17,959	—
1-D-H-U-2	1	52.6	363	17,940	—
1-D-M-U-3	1	34.7	239	63,221	—
1-D-M-U-4	1	34.7	239	59,773	—
1-D-L-U-5	1	24.9	172	246,744	LFC + 10 %
1-D-L-U-6	1	21.5	148	2,977,599	runout LFC + 5 %
1-D-L-U-7	1	22.9	158	493,574	LFC + 7.5 %
1-D-H-O-1	2	52.6	363	17,628	—
1-D-H-O-2	2	34.7	239	16,672	—
1-D-M-O-3	2	34.7	239	95,905	—
1-D-M-O-4	2	34.7	239	92,145	—
1-D-L-O-5	2	17.9	123	3,383,336	runout
1-D-L-O-6	2	21.5	148	7,899,730	runout LFC + 5 %
1-D-L-O-7	2	24.9	172	369,586	LFC + 10 %
1-D-L-O-8	2	22.9	158	641,584	LFC + 7.5 %

Table 27—S-N Fatigue Test Results for 1-in. Bolts in SW+CP (Phase II)

Specimen ID	Heat	Stress Range, Δσ		Cycles to Failure	Comments
		ksi	MPa		
1-W-H-O-1	2	52.6	363	11,752	—
1-W-H-O-2	2	52.6	363	12,418	—
1-W-H-O-3	2	52.6	363	12,850	—
1-W-M-O-4	2	34.7	239	37,008	—
1-W-M-O-5	2	34.7	239	25,283	—
1-W-M-O-6	2	34.7	239	34,613	—
1-W-L-O-7	2	17.9/20.7	123/143	414,607	Increased to LFC + 4 % after 381,298 cycles
1-W-L-O-8	2	17.9/21.5	123/148	618,490	Increased to LFC + 5 % after 567,405 cycles, stopped without fracture
1-W-L-O-9	2	21.5	148	128,960	LFC + 5 %
1-W-L-O-10	2	21.5	148	164,318	LFC + 5 %
1-W-L-O-11	2	22.5	155	132,907	Wrong max. and min. load, discarded result
1-W-L-O-12	2	20.7	143	719,682	LFC + 4 %, stopped without fracture
1-W-H-U-1	1	52.6	363	13,996	—
1-W-H-U-2	1	52.6	363	13,240	—
1-W-H-U-3	1	52.6	363	12,422	—
1-W-M-U-4	1	34.7	239	33,575	—
1-W-M-U-5	1	34.7	239	29,435	—
1-W-M-U-6	1	34.7	239	25,395	—
1-W-L-U-7	1	21.5	148	266,357	LFC + 5 %
1-W-L-U-8	1	21.5	148	154,412	LFC + 5 %
1-W-L-U-9	1	21.5	148	504,542	LFC + 5 %

Table 28—S-N Fatigue Test Results for 3-in. Bolts in Air (Phase II)

Specimen ID	Heat	Stress Range, Δσ		Cycles to Failure	Comments
		ksi	MPa		
3-D-H-U-1	1	52.6	363	11,445	—
3-D-H-U-2	1	52.6	363	11,370	—
3-D-M-U-3	1	34.7	239	34,172	—
3-D-M-U-4	1	34.7	239	35,877	—
3-D-L-U-5	1	17.9	172	460,566	—
3-D-L-U-6	1	17.9	172	720,260	—
3-D-L-U-7	1	17.9	172	479,181	—
3-D-H-O-1	2	52.6	363	10,017	—
3-D-H-O-2	2	52.6	363	10,638	—
3-D-M-O-3	2	34.7	239	33,264	—
3-D-M-O-4	2	34.7	239	33,712	—
3-D-L-O-5	2	17.9	123	225,637	—
3-D-L-O-6	2	17.9	123	212,144	—
3-D-L-O-7	2	17.9	123	252,474	—

Table 29—S-N Fatigue Test Results for 3-in. Bolts in SW+CP (Phase II)

Specimen ID	Heat	Stress Range, Δσ		Cycles to Failure	Comments
		ksi	MPa		
3-W-H-U-1	1	52.6	363	10,248	—
3-W-H-U-2	1	52.6	363	10,822	—
3-W-H-U-3	1	52.6	363	11,015	—
3-W-M-U-4	1	34.7	239	28,626	—
3-W-M-U-5	1	34.7	239	28,038	—
3-W-M-U-6	1	34.7	239	30,828	—
3-W-L-U-7	1	17.9	123	748,367	Stopped without fracture, runout
3-W-L-U-8	1	17.9	123	0	Stopped due to technical issues with the test frame
3-W-L-U-9	1	17.9	123	136,365	—
3-W-L-U-10	1	17.9	123	367,342	—
3-W-H-O-1	2	52.6	363	10,322	—
3-W-H-O-2	2	52.6	363	10,428	—
3-W-H-O-3	2	52.6	363	10,623	—
3-W-M-O-4	2	34.7	239	27,838	—
3-W-M-O-5	2	34.7	239	27,621	—
3-W-M-O-6	2	34.7	239	27,275	—
3-W-L-O-7	2	17.9	123	109,373	—
3-W-L-O-8	2	17.9	123	107,181	—
3-W-L-O-9	2	17.9	123	125,140	—

5.2.8 S-N Fatigue Curves in Air and in SW+CP Environments (Phase II)

Figures 13 and 14 show the S-N fatigue curves obtained for the 1-in. bolts in air and in an SW+CP environment. The plots also show the mean and mean $-t_p$ * SD. Following the same approach of Phase I, the statistical analysis was performed in accordance with requirements of ASTM E739. The test results that showed runouts were excluded in the regression analysis.

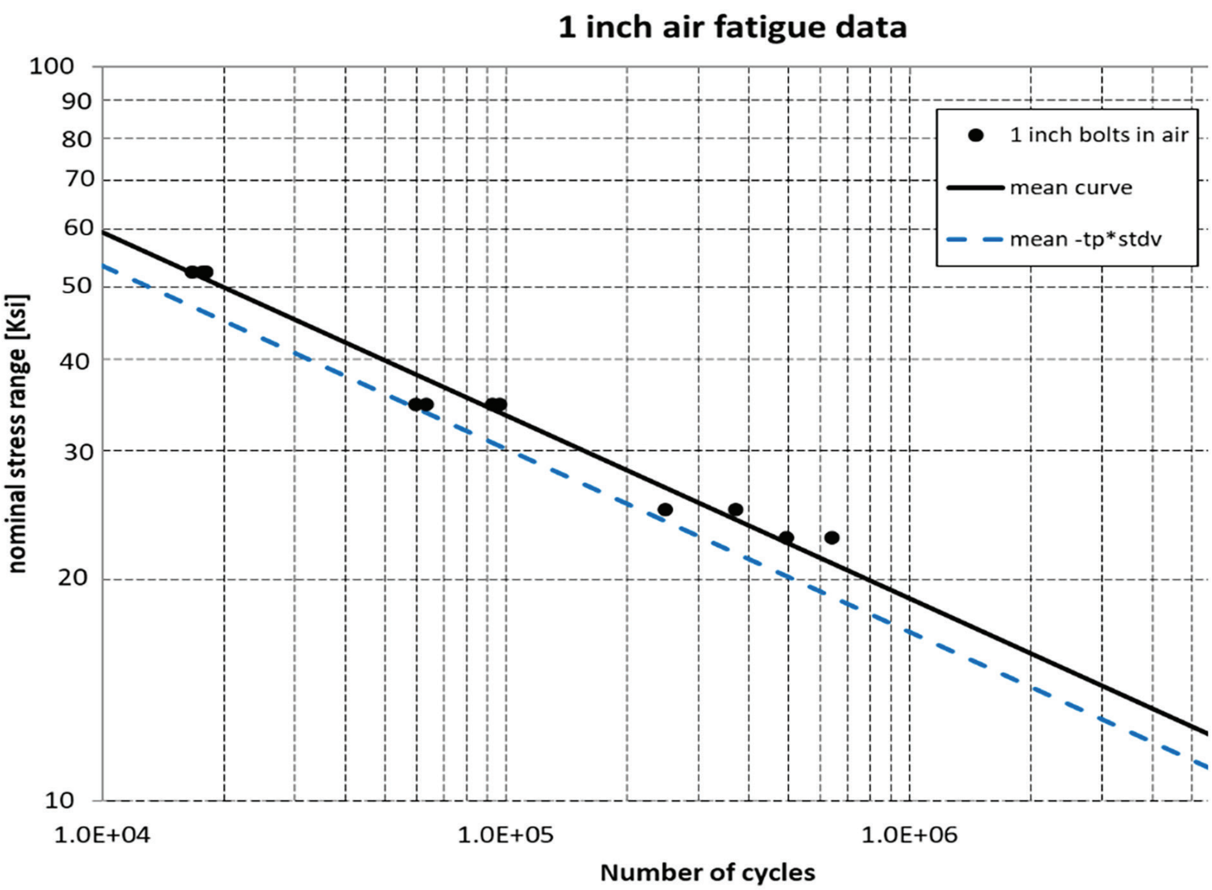

1 in. Air Data	Phase II, Disregarding Runouts Free Regression
m =	4.01
$\log a_1$ (mean)	11.110
StD ($\log \overline{a_1}$)	0.091
Tp (12 test data)	2.201
Mean-tp*stdv	10.910

Figure 13—S-N Fatigue Curve for 1-in. Bolts in Air (Phase II)

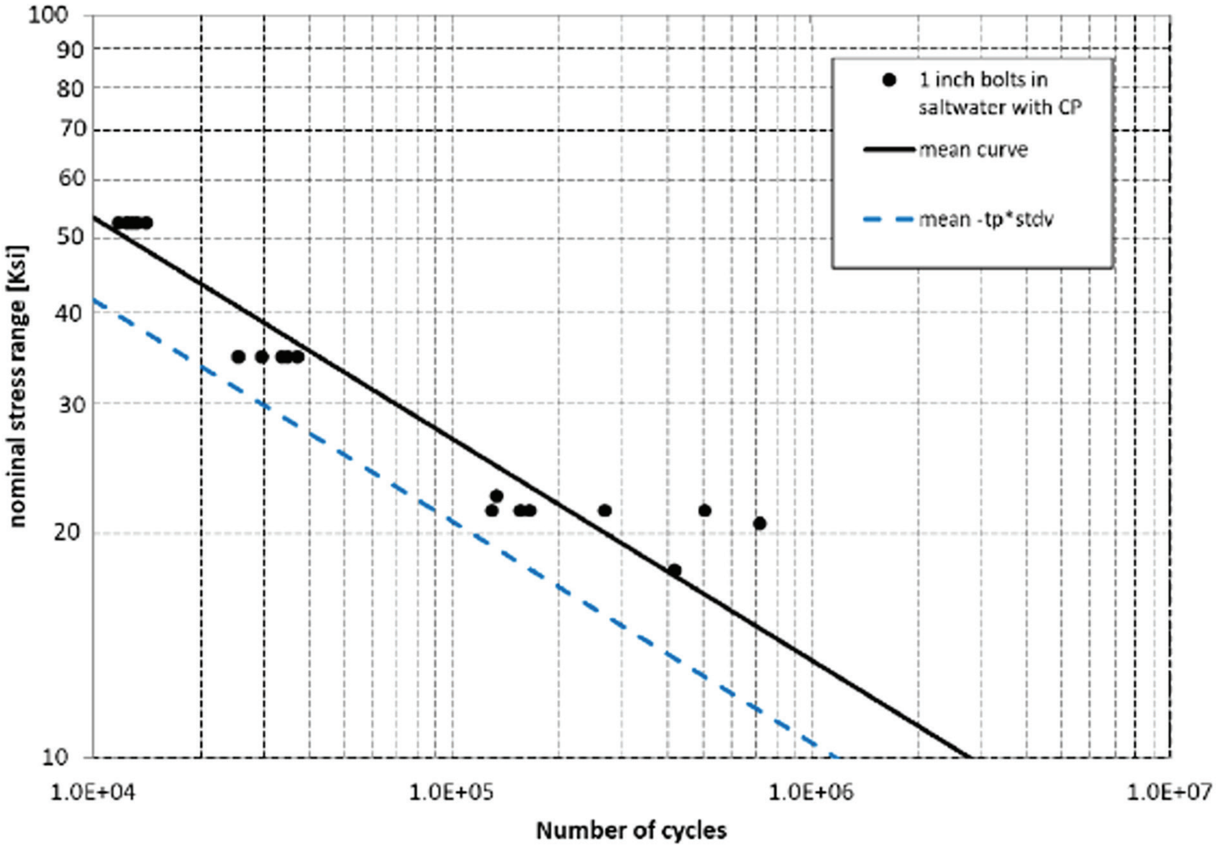

1 in. SW + CP Data	Phase II, Disregarding Runouts Free Regression
m =	3.20
$\log a_1$ (mean)	9.541
StD ($\log \overline{a_1}$)	0.155
Tp (18 test data)	2.120
Mean-tp*stdv	9.210

Figure 14—S-N Fatigue Curve for 1-in. Bolts in an SW+CP Environment (Phase II)

Figure 15 compares the test results for the 1-in. bolts in air and in SW+CP. The effect of hydrogen uptake on the 1-in. bolts is illustrated by the lower fatigue life in SW+CP as compared to in air at the same stress ranges. The hydrogen charging effects in fatigue life were more pronounced at LFC, which led to a steeper slope of the SW+CP fatigue curve.

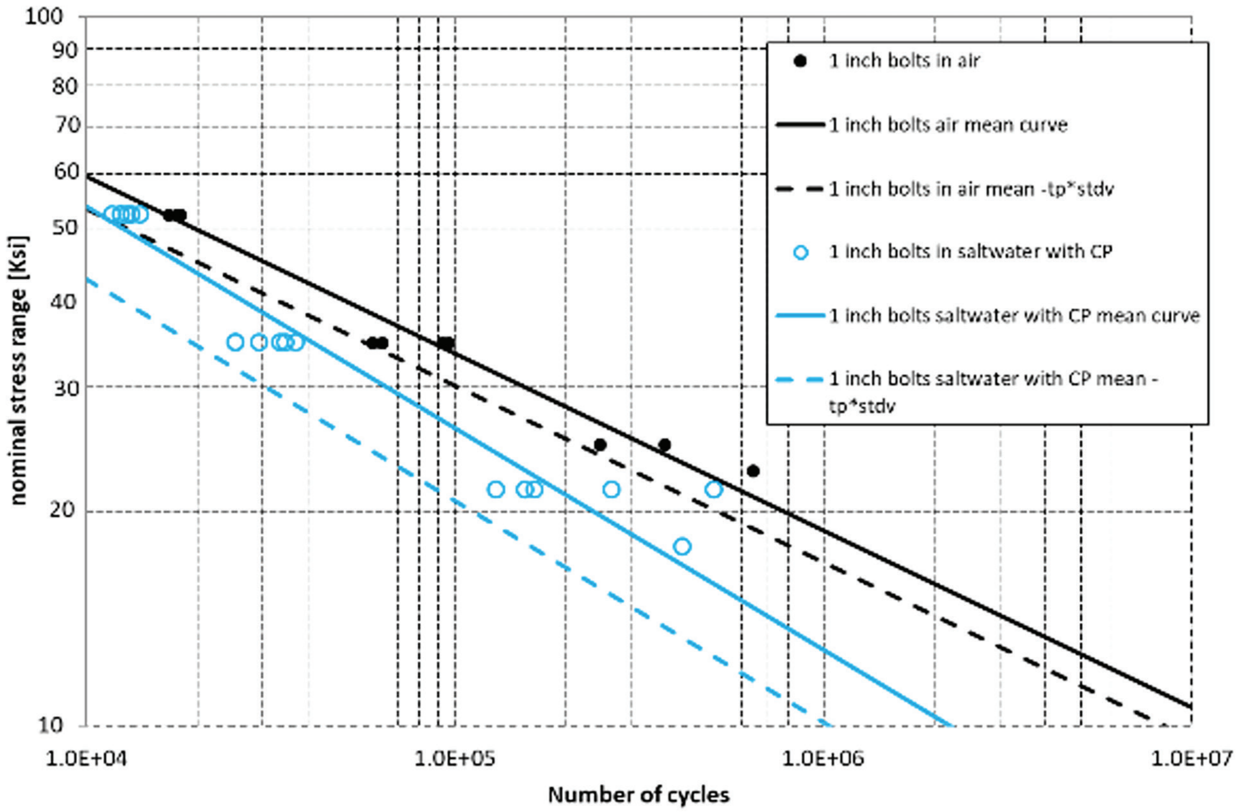

Figure 15—S-N Fatigue Test Results for 1-in. Bolts in Air and SW+CP (Phase II)

Figures 16 and 17 show the S-N fatigue curves for the 3-in. bolts in air and in an SW+CP environment, respectively.

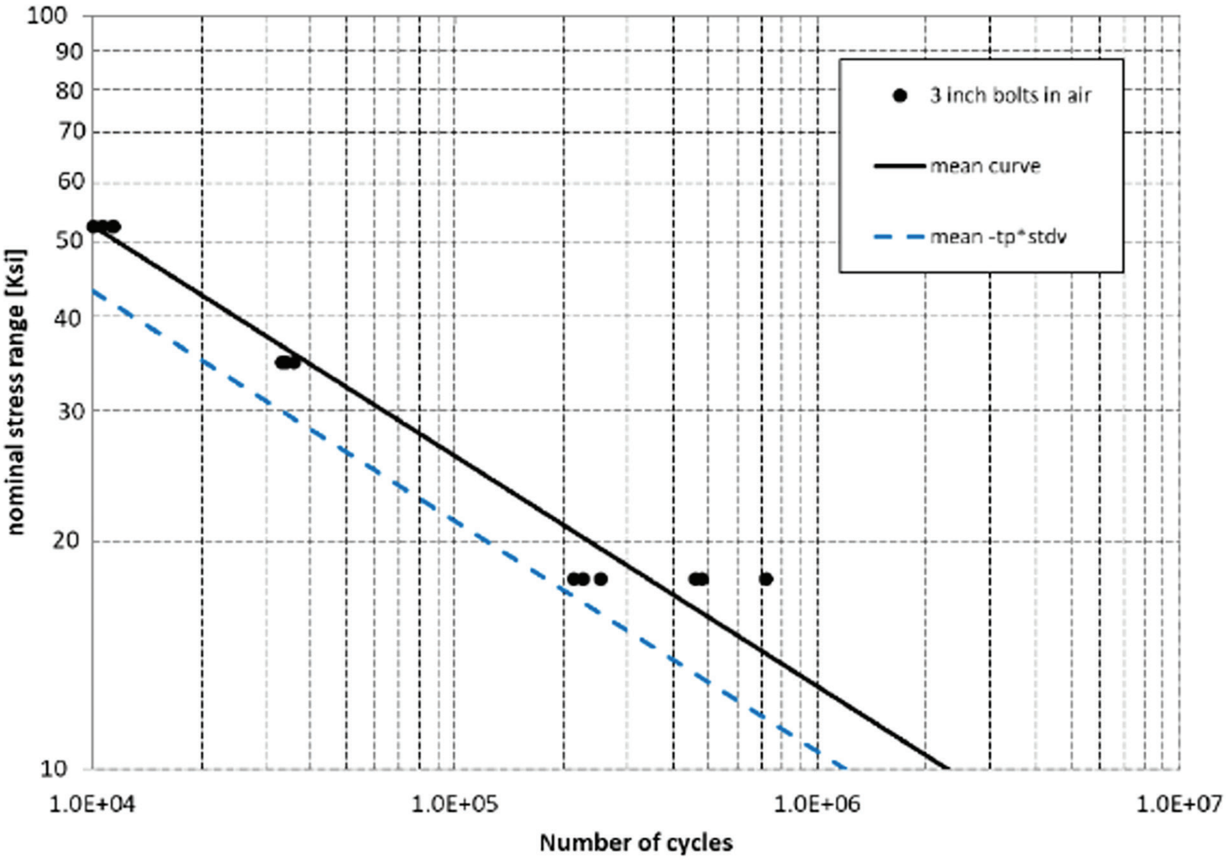

3 in. Air Data	Phase II, Disregarding Runouts Free Regression
m =	3.27
$\log a_1$ (mean)	9.629
StD ($\log \overline{a_1}$)	0.140
Tp (14 test data)	2.179
Mean-tp*stdv	9.323

Figure 16—S-N Fatigue Curve for 3-in. Bolts in Air (Phase II)

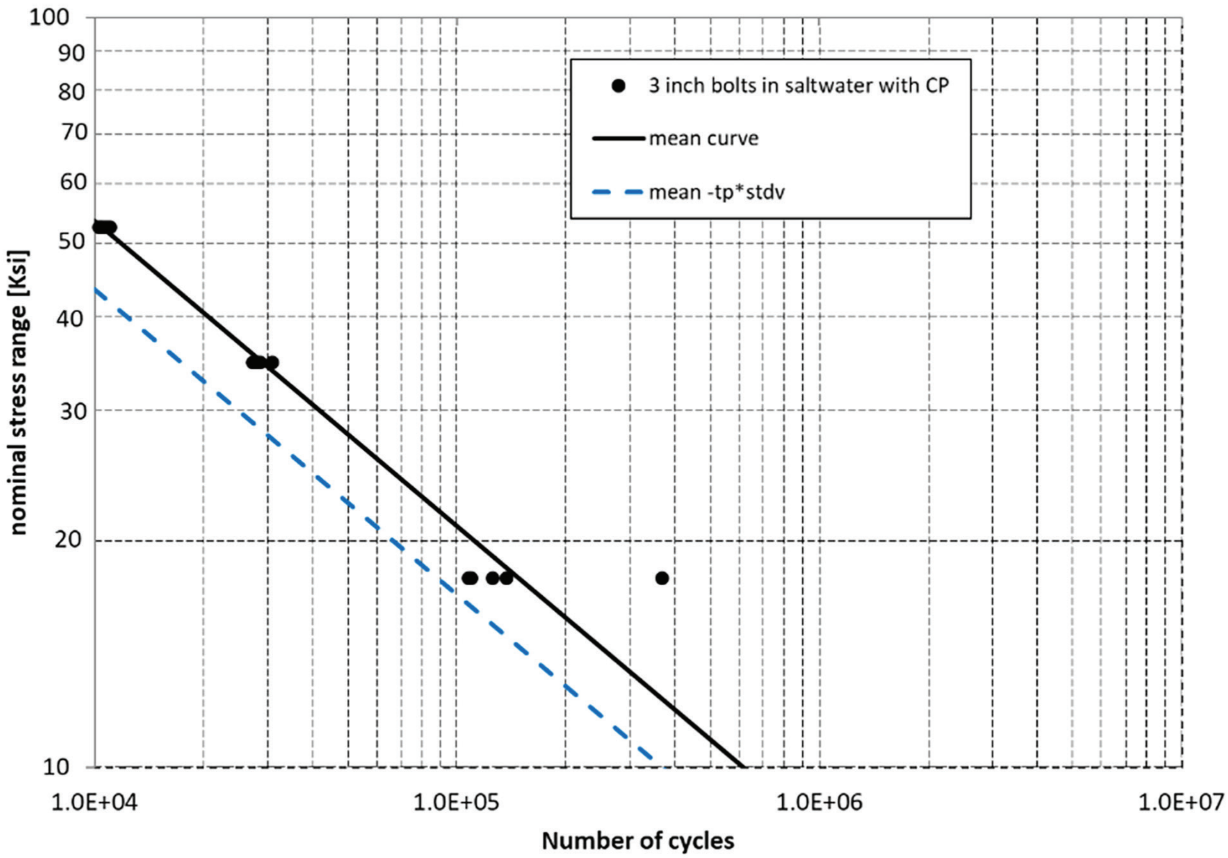

3 in. SW + CP Data	Phase II, Disregarding Runouts Free Regression
m =	2.46
$\log a_1$ (mean)	8.244
StD ($\log \overline{a_1}$)	0.113
Tp (17 test data)	2.132
Mean-tp*stdv	8.008

Figure 17—S-N Fatigue Curve for 3-in. Bolts in an SW+CP Environment (Phase II)

Figure 18 compares the test results for the 3-in. bolts in air and in an SW+CP environment. At HFC, the difference in fatigue lives in air and SW+CP environments are insignificant, indicating that at HFC, the fatigue life of 3-in. bolts in an SW+CP environment is dominated by bolt stiffness and stress concentration factor at the thread root of the bolting rather than hydrogen uptake. In addition, hydrogen uptake and transport in the material is a time-dependent phenomenon and, hence, a lesser effect of hydrogen embrittlement due to duration of the test at HFC and MFC is typically observed.

At LFC, the difference between air and SW+CP is more pronounced, with an SW+CP environment showing lower overall fatigue lives due to availability of time for hydrogen uptake and transport to the fracture process zone at or beneath the thread roots. At LFC, the scatter of the test results in air and an SW+CP environment is higher than MFC and HFC, but overall fatigue lives in SW+CP appears to be lower due to hydrogen uptake and embrittlement. In general, the 3-in. bolts mean curve in an SW+CP environment exhibits a steeper slope.

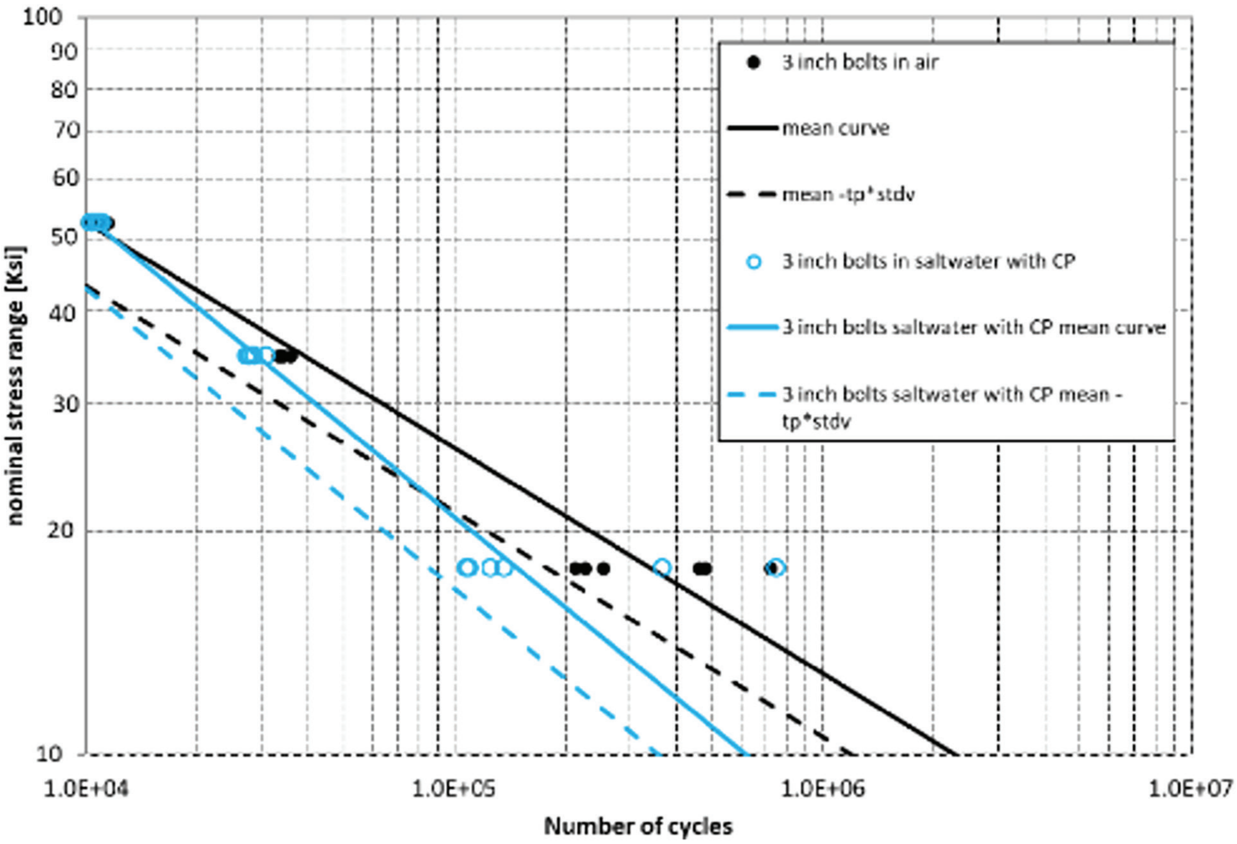

Figure 18—S-N Fatigue Test Results for 3-in. Bolts in Air and SW+CP (Phase II)

Figures 19 and 20 compare the S-N fatigue design curves for the 1-in. and 3-in. bolts in air and in an SW+CP environment, respectively. Figure 19 shows that in air, the 3-in. bolt exhibits a lower fatigue capacity at each stress range and steeper slope as compared to the 1-in. bolts. This is attributed to the higher stiffness and stress concentration factor at the thread roots of the 3-in. bolts.

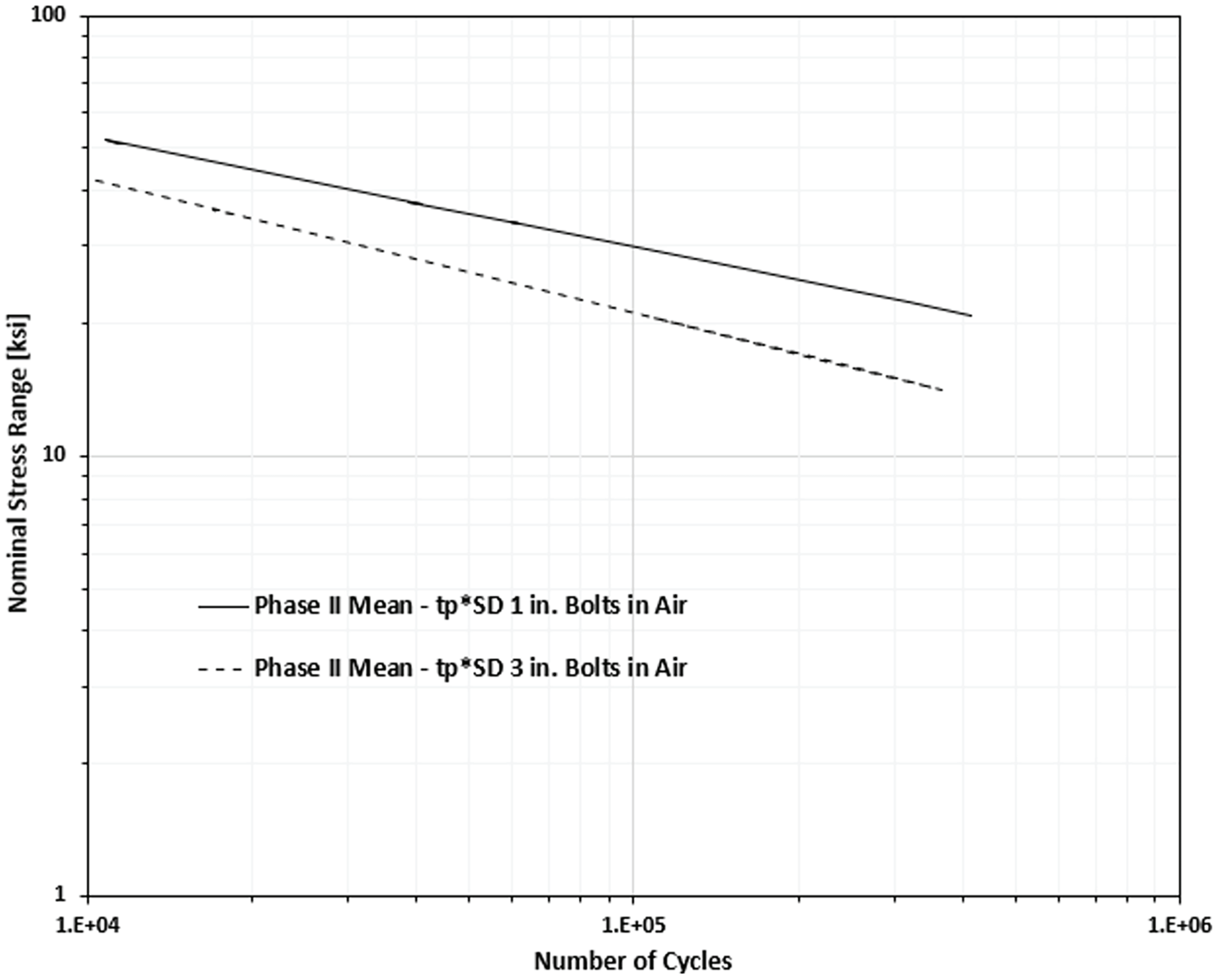

Figure 19—Comparison of the 1-in. and 3-in. Bolt S-N Fatigue Curves in Air (Phase II)

A similar trend is observed in Figure 20 for the 1-in. and 3-in. bolts tested in an SW+CP environment—except at HFC, the difference in fatigue lives appear to be minimal. Besides stiffness and stress concentration effects discussed for in air fatigue curves comparison, hydrogen uptake and embrittlement also plays a role in an SW+CP environment. The hydrogen embrittlement effect on 1-in. bolts are more pronounced, shifting the curve toward the 3-in. bolts curve.

This indicates that at the HFC, the difference in fatigue lives (if any) between the 1-in. and 3-in. bolts in SW+CP are dominated by the bolt stiffness and stress concentration factors at the thread roots. At LFC, fatigue lives seem to be dominated by atomic hydrogen diffusion and transport to the fracture process zone at or beneath the thread roots. The results show that this process is more prevalent as the thickness of the bolt increases, leading to lower fatigue lives and, hence, steeper design fatigue curves at the same nominal applied stress range.

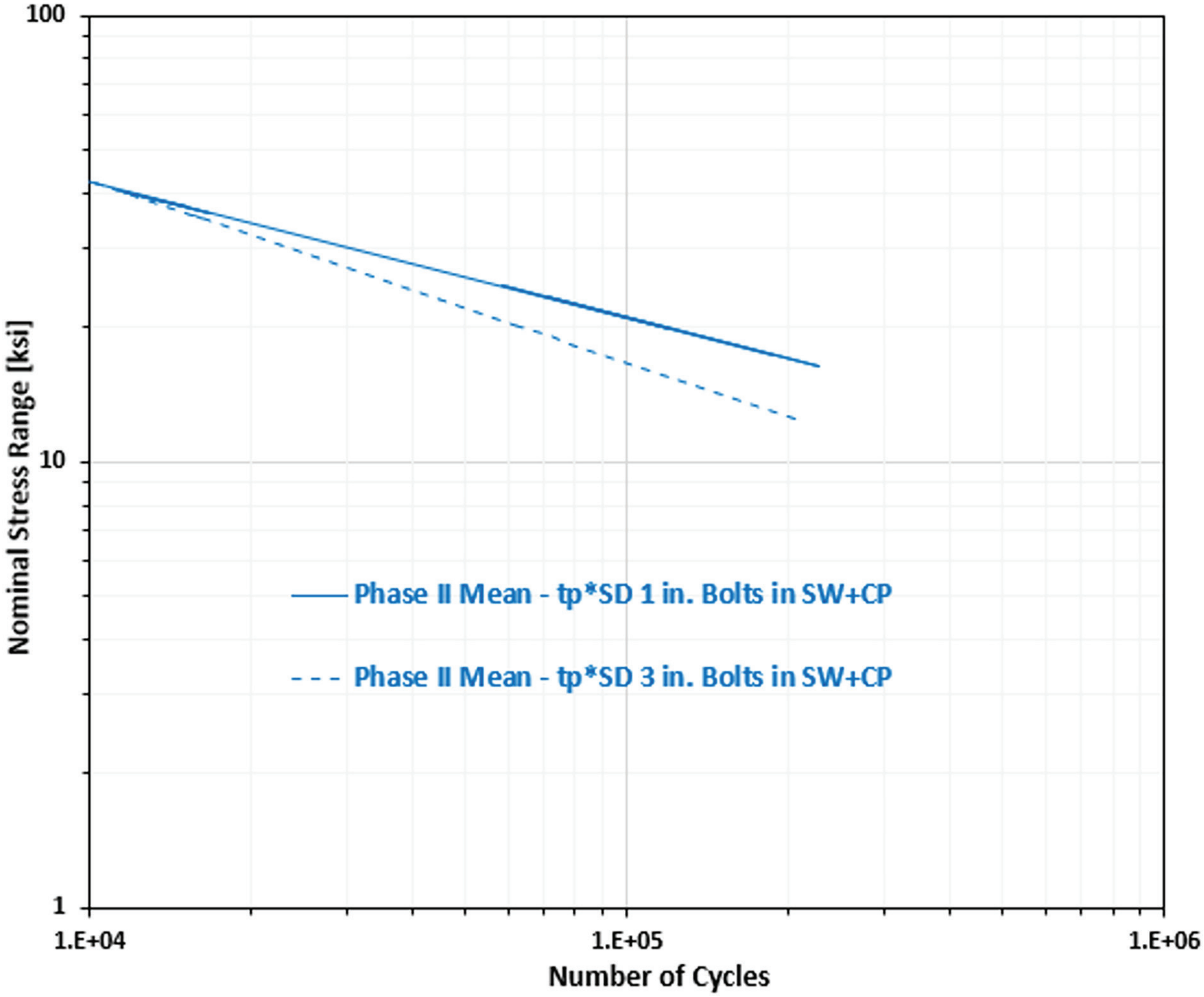

Figure 20—Comparison of the 1-in. and 3-in. Bolt S-N Fatigue Curves in SW+CP (Phase II)

Based on the Phase II S-N fatigue curves for the 1-in. and 3-in. bolts in air and an SW+CP environment, Table 30 provides a knock-down factor at different stress ranges for the two bolt sizes.

Table 30—Knock-Down Factors for SW+CP/Air Environments at Applied Stress Ranges (Phase II)

Stress Range $\Delta\sigma$		1 in.	3 in.
ksi	MPa		
52.6	362.4	0.73	0.97
34.7	239.1	0.40	0.83
21.5	148.1	0.06 [a]	—
17.9	123.3	—	0.43

[a] No ambient air failures.

5.2.9 Post-Test Evaluation (Phase II)

5.2.9.1 General

Upon completion of each S-N test, the bolts were evaluated, and pictures of their fracture surfaces were taken and documented on a result sheet along with other information specific to each bolt. A few fractured bolts from each heat and size were selected to be studied further.

5.2.9.2 Hardness Measurements

After completion of the S-N tests, six (6) bolts were selected for hardness measurement. This included three (3) 1-in. bolts (1-W-L-O-9, 1-W-M-U-6, 1-W-M-O-5) and three (3) 3-in. bolts (3-W-L-O-8, 3-W-L-U-7, 3-W-L-U-9). All the selected bolts were fatigue tested in an SW+CP environment. The purpose was to determine if any work/strain hardening took place due to the stresses at the first and second engaged threads as well as hydrogen concentration at these locations.

Hardness measurements were conducted using the Vickers (HV1 and HV10) scale. Measured Vickers hardnesses were then converted to Rockwell C (HRC) per ASTM E140-12b (reapproved 2019), Table 1. Figure 21 shows the location of hardness measurements, a), and the indent number allocated to each hardness reading, b), for both bolt sizes.

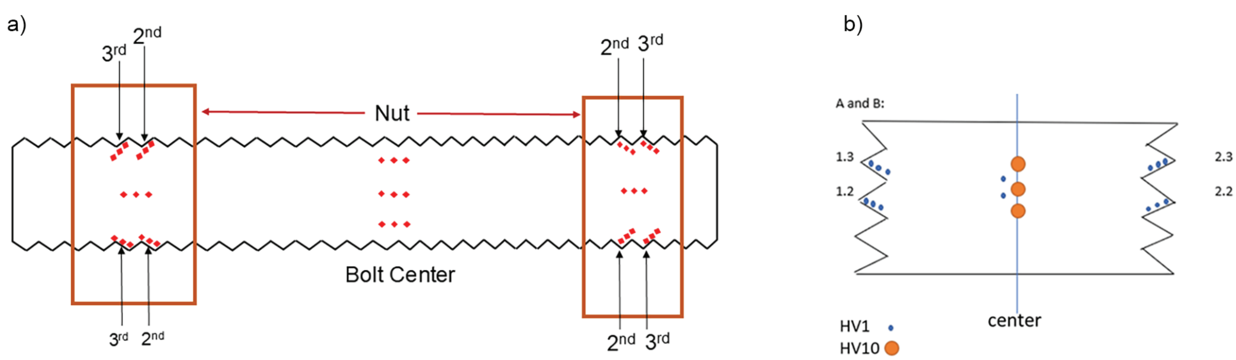

Key

a) Vickers hardness testing location

b) indent number allocated to each hardness reading

Figure 21—Schematics of Hardness Test Locations (Phase II)

Table 31 and Table 32 show both the HV1 and HV10 hardness measurements as well as the converted HRC values for the 1-in. and 3-in. bolts (Phase II).

Table 31—Measured HV1 and HV10 Hardness and Converted HRC Values for the 1-in. Bolts (Phase II)

1 in.	Indent Number	1-W-L-O-9 1st Thread		1-W-L-O-9 2nd Thread		1-W-M-U-6 1st Thread		1-W-M-U-6 2nd Thread		1-W-M-O-5 1st Thread		1-W-M-O-5 2nd Thread	
		HV1	HRC	HV1	HRC	HV1	HRC	HV1	HRC	HV1	HRC	HV1	HRC
1.2 (A)	1	271	26	269	26	285	28	292	29	276	26	268	25
	2	273	26	274	26	285	28	298	30	271	26	276	27
	3	273	26	269	26	293	29	284	28	281	27	268	25
1.3 (A)	4	271	26	272	26	285	28	292	29	275	26	275	26
	5	273	26	276	26	290	29	279	27	272	26	277	27
	6	273	26	273	26	301	30	292	29	277	27	274	26
2.2 (B)	7	279	27	277	27	289	28	295	29	272	26	271	26
	8	279	27	275	26	292	29	290	29	280	27	277	27
	9	279	27	271	26	289	28	285	28	276	26	275	26
2.3 (B)	10	269	25	271	26	287	28	291	29	273	26	268	25
	11	276	26	275	26	291	29	278	27	275	26	275	26
	12	276	26	272	26	289	28	282	27	273	26	274	26
Average		274	26	273	26	290	29	289	29	275	26	273	26
Center HV10	13	271	26	263	25	287	28	275	26	267	26	266	25
	14	271	26	263	25	284	28	278	27	270	26	269	26
	15	270	26	262	25	287	28	281	27	271	26	270	26
Average		271	26	263	25	286	28	278	27	269	26	268	26

Table 32—Measured HV1 and HV10 Hardness and Converted HRC Values for the 3-in. Bolts (Phase II)

1 in.	Indent Number	3-W-L-O-8 1st		3-W-L-O-8 2nd Thread		3-W-L-U-9 1st Thread		3-W-L-U-9 2nd Thread		3-W-L-U-7 1st Thread		3-W-L-U-7 2nd Thread	
		HV1	HRC	HV1	HRC	HV1	HRC	HV1	HRC	HV1	HRC	HV1	HRC
1.2 (A)	1	284	27	312	31	289	28	302	30	284	27	294	29
	2	283	27	291	28	290	28	280	27	304	30	291	28
	3	277	26	293	28	281	27	298	29	279	27	306	30
1.3 (A)	4	290	28	301	29	277	26	307	30	315	31	288	29
	5	272	26	288	28	286	28	295	29	285	27	302	30
	6	276	26	293	28	285	27	296	29	280	27	295	29
2.2 (B)	7	281	27	309	30	278	26	296	29	284	27	292	28
	8	285	27	295	29	289	28	285	27	277	26	292	28
	9	280	27	291	28	285	27	292	28	275	26	290	28
2.3 (B)	10	276	26	305	30	277	26	312	31	278	26	278	26
	11	279	27	292	28	282	27	300	29	290	28	287	28
	12	285	27	298	29	285	27	303	30	286	27	276	26
Average		281	27	297	29	284	27	297	29	286	28	291	28
Center HV10	13	285	27	284	27	283	27	288	28	284	27	284	27
	14	289	28	282	27	286	28	285	27	284	27	281	27
	15	288	28	274	26	285	27	282	27	280	27	278	26
Average		287	28	280	27	285	27	285	27	283	27	281	27

5.2.9.3 Microstructure Evaluation

For microstructural examination, the same 1-in. and 3-in. bolts for hardness measurements were used. Cross-sectional samples were cut from each bolt, polished, and etched to reveal the microstructure. The microstructures were examined with an optical microscope, and photomicrographs were taken at various magnifications.

Figure 22 shows the microstructure at the center and the thread of bolt sample 1-W-M-U-6 at 200X. The microstructure at the center of the bolt is primarily tempered martensite with light banding. The tempered martensite with light banding was observed from both the center and the thread areas for all 1-in. bolts examined.

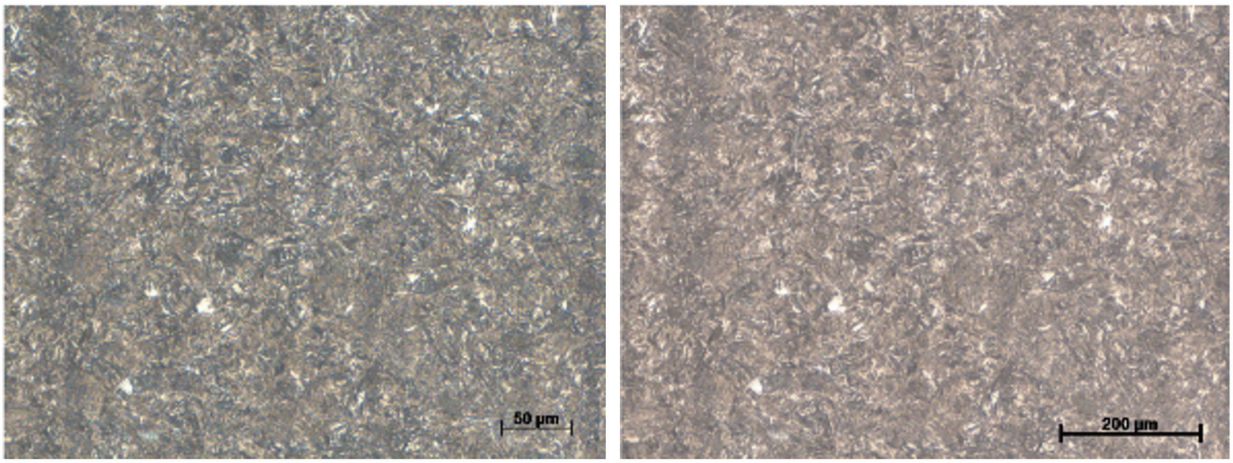

a) b)

Key
a) center
b) thread

Figure 22—Optical Microscope Photomicrograph (Phase II)

The microstructure of the 3-in. bolts also included tempered martensite with light banding, but it also included some retained austenite. Figure 23 shows the microstructure of the 3-in. bolt identified as 3-W-L-O-8 at 200X. The picture was taken from a sample cut from the middle of the bolt in the center. The light-colored phase at the center of Figure 23 was identified as retained austenite.

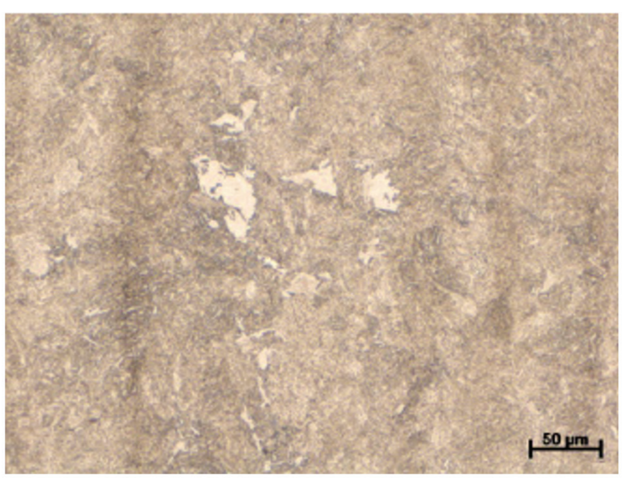

Figure 23—Optical Microscope Photomicrograph (Phase II)

The retained austenite was identified using SEM and energy-dispersive X-ray spectroscopy (EDS) mapping. The result of mapping for different elements is shown in Figure 24.

The elemental mapping shows that the elements are randomly distributed in the light-colored phase and surrounding area, which was mostly tempered martensite. This suggests the light-colored phase is retained austenite that did not transform to martensite during quenching.

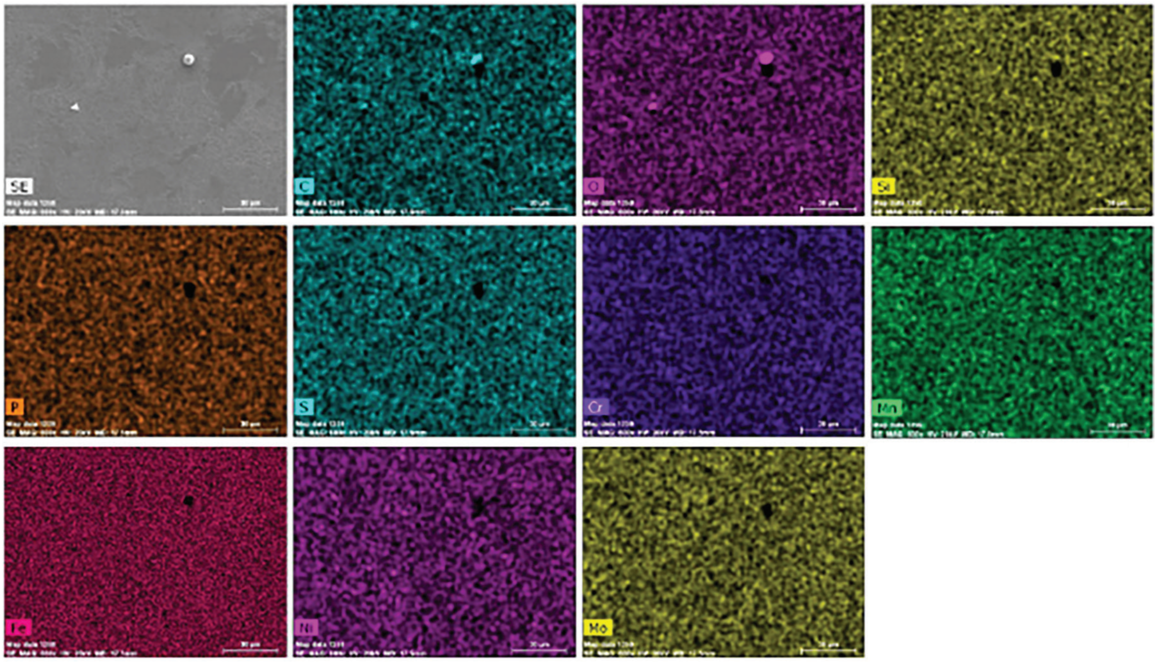

Figure 24—EDS Mapping of the Light-Colored Phase Observed (or Described) in Figure 23

5.2.9.4 Thread Root Roughness Profile

As shown by the S-N fatigue curves in air and in SW+CP developed in Phase II, large scatter in fatigue lives were observed at the lowest applied nominal stress range (LFC) for both 1-in. and 3-in. bolts. Additionally, the 3-in. bolts supplied by one of the suppliers consistently showed higher fatigue lives at LFC as compared to the second bolting supplier. As a result, the thread root surface conditions of several 3-in. bolts from both suppliers tested at LFC in air were evaluated by SEM. For this objective, 10 cm to 15 cm (4 in. to 6 in.) samples from the intact thread regions of tested bolts in air were cut to ensure that the threads were not altered due to mechanical contact with the nut threads.

Figure 25 compares the thread root surface conditions of the 3-in. bolts from the two heats tested in air at LFC ($\Delta\sigma$ = 17.9 ksi). The bolts were identified as 3-D-L-O-6 (N_f = 212,144 cycles), and 3-D-L-U-6 (N_f = 720,260 cycles), respectively. These SEM photomicrographs show that the thread root surface roughness of the bolts from the two heats varies from one heat to the other.

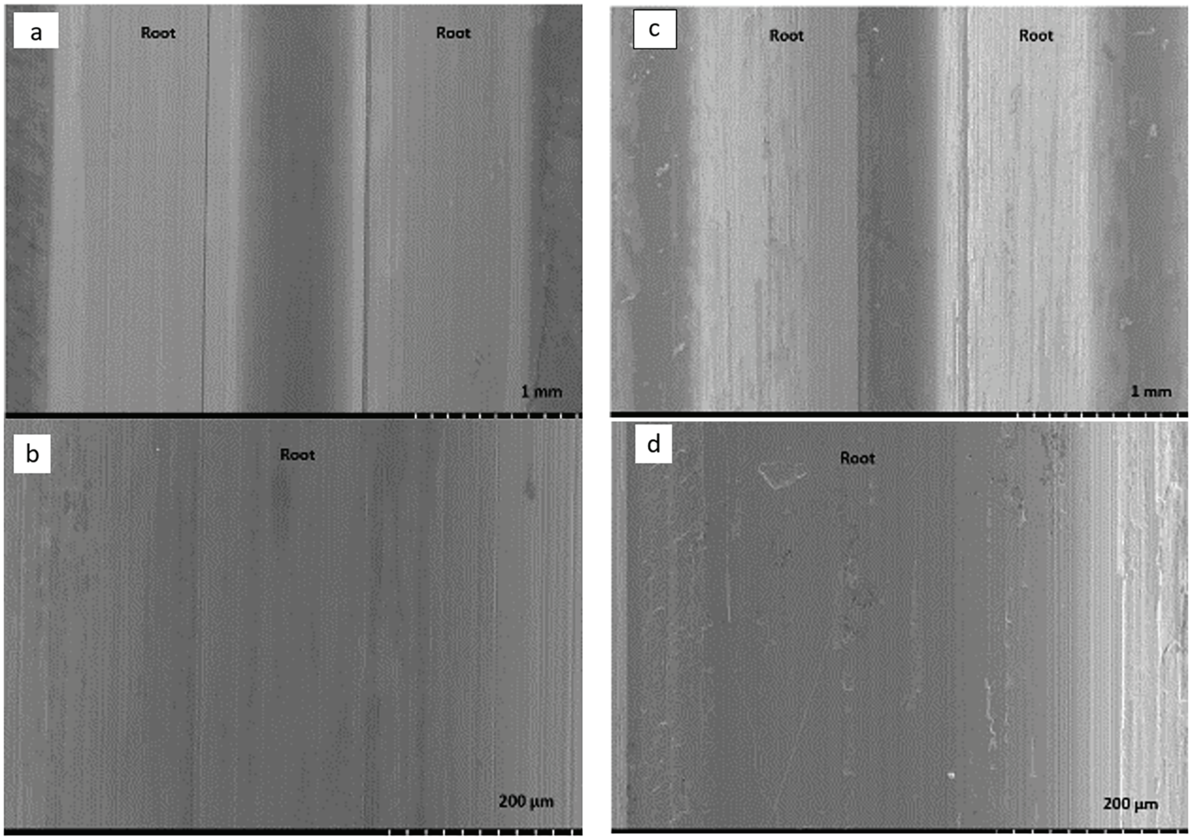

Key
a) and b) thread root roughness – Heat 1
c) and d) thread root roughness – Heat 2

Figure 25—SEM Photomicrograph Taken at Low Magnification for 3-in. Bolts

These results illustrate that even though both suppliers provided API 20E BSL-3-conforming 3-in. bolts, thread root surface roughness has made a difference in bolting fatigue life at LFC when tested in air. The S-N test results for 3-in. bolts in air illustrate that even though both Heat 1 and Heat 2 were supplied in accordance with API 20E BSL-3 requirements, thread root surface roughness has made a difference in bolting fatigue life at LFC.

6 Conclusions

Full-scale S-N fatigue testing of low-alloy steel bolting of 1-in., 2-in., and 3-in. in Phase I and 1-in. and 3-in. in Phase II in air and SW+CP environments provided valuable data that can be used for the applicable designs. The main conclusions are the following:

a) The bolting fatigue life decreases with increasing the bolt size. This is due to increased stiffness and increased root radius stress concentration factor with increasing bolt size [13].

b) Fatigue testing of 1-in. bolts in air and at the low stress range exhibited runouts in both phases, indicating an endurance limit that varies with mean stress. The endurance limit in air seems to be near 17 ksi and 20 ksi for Phase I and Phase II, respectively.

c) The fatigue reduction factor for SW+CP is affected by both bolt size and stress ranges. The higher the alternating stress and the larger the bolt, the less the reduction factor in environment. This is attributed to atomic hydrogen diffusion and transport being more dominant at the lower alternating stress levels.

d) The log-log plot of the slope for the fatigue curves for the SW+CP tests is steeper than the slope of the curve for the ambient air tests. This again is due to the influence of the atomic hydrogen diffusion and transport at lower alternating stress ranges.

e) Phase II testing results showed that the knock-down factor due to SW under CP influence is less for the 3-in. bolts than for the 1-in. bolts.

f) Both 1-in. and 3-in. bolts show a mean stress dependency in both environments. In Phase II, higher fatigue lives were obtained due to lower mean stress than in Phase I, where the mean stress was higher.

g) All bolts demonstrated no susceptibility to shear failure of the threads from testing and post-test evaluation. All the bolt failures observed were due to crack initiation at the first engaged thread root in bolt thread, which propagated radially through the cross section of the bolt (tensile type failure).

h) Although bolting for Phase I and Phase II was conforming with API 20E BSL-3 requirements, differences in bolting thread root roughness appeared to contribute to a wider scatter in fatigue lives at the lowest applied nominal stress range in air.

Bibliography

[1] API Specification 17D:2011, *Design and Operation of Subsea Production Systems—Subsea Wellhead and Tree Equipment*

[2] API Specification 6A, *Specification for Wellhead and Christmas Tree Equipment*

[3] *API Specification 16A,Specification for Drill-through Equipment*

[4] API Specification 20E, *Alloy and Carbon Steel Bolting for Use in the Petroleum and Natural Gas Industries*

[5] ASME B1.1-2003, *Unified Screw Threads (UN and UNR Thread Form)*

[6] *DNV-RP-C203,Fatigue Design of Offshore Steel Structures, Edition 2019*

[7] Counts, W., Johnson, W.S., Chang, J., *Assessing Life Prediction Methodologies for Fasteners Under Bending Loads,* ASTM STP 1391, Structural Integrity of Fasteners, 2nd Vol, 2000, pp. 3–15

[8] ASTM A194/A194M, *Standard Specification for Carbon Steel, Alloy Steel, and Stainless Steel Nuts for Bolts for High Pressure of High Temperature Service, or Both*

[9] ASTM A320/A320M, *Standard Specification for Alloy-Steel and Stainless Steel Bolting for Low-Temperature Service*

[10] ISO 23788:2012, *Metallic Materials—Verification of the Alignment of Fatigue Testing Machines*

[11] ASTM E739, *Standard Practice for Statistical Analysis of Linear of Linearized Stress-Life (S-N) and Strain-Life (ε-N) Fatigue Data*

[12] ASTM E140, *Standard Hardness Conversion Tables for Metals Relationship Among Brinell Hardness, Vickers Hardness, Rockwell Hardness, Superficial Hardness, Knoop Hardness, and Scleroscope Hardness*

[13] Lim, J. I., Bunch, P., Han, Y., Offshore Technology Conference, OTC-27820-MS, May 2017

American
Petroleum
Institute

200 Massachusetts Avenue, NW
Suite 1100
Washington, DC 20001-5571
USA

202-682-8000

Additional copies are available online at www.api.org/pubs

Phone Orders:	1-800-854-7179	(Toll-free in the U.S. and Canada)
	303-397-7956	(Local and International)
Fax Orders:	303-397-2740	

Information about API publications, programs and services is available on the web at www.api.org.

Product No. G21TR202